



This is to certify that the

thesis entitled

SENSITIVITY OF FLOW RATE CALCULATIONS TO THE RHEOLOGICAL PROPERTIES OF HERSCHEL-BULKLEY FLUIDS

presented by

Ibrahim Omer Mohamed

has been accepted towards fulfillment of the requirements for

M.S. degree in Agricultural Engineering

Major professor

Dr. James F. Steffe

Date_August 10, 1984

O-7639

MSU is an Affirmative Action/Equal Opportunity Institution



RETURNING MATERIALS:
Place in book drop to remove this checkout from your record. FINES will be charged if book is returned after the date stamped below.

SENSITIVITY OF FLOW RATE CALCULATIONS TO THE RHEOLOGICAL PROPERTIES OF HERSCHEL-BULKLEY FLUIDS

Ву

Ibrahim Omer Mohamed

THESIS

Submitted to
Michigan State University
in partial fulfillment of the requirements
for the degree of

MASTER OF SCIENCE

Department of Agricultural Engineering

1984

ABSTRACT

SENSITIVITY OF FLOW RATE CALCULATIONS TO THE RHEOLOGICAL PROPERTIES OF HERSCHEL-BULKLEY FLUIDS

By

Ibrahim Omer Mohamed

The purpose of this study is to show the problems that might be encountered when unreliable rheological data are used to estimate flow rate. The root sum square formula is used to show the sensitivity of flow rate calculations to the magnitude and precision of the rheological parameters describing Herschel-Bulkley fluids. The analysis was performed for laminar flow using the mixing length method to establish laminar-transional flow.

The result of the analysis shows that the error in flow rate increased with decreases in the magnitude of the flow behavior index. Error in the flow behavior index of ± 0.0001, ± .001 and ± .01 has no significant effect on the error in flow rate. Flow rate error is not influenced by the magnitude of the consistency coefficient for the range investigated; however, the error does increase with increasing error in the consistency coefficient. The magnitude of the yield stress has a strong effect on the error in flow rate when the shear stress at the wall approaches the yield stress. The error in yield stress was found to be the most important factor in causing error in flow rate.

Approved	
-	Major Professor
Approved _	
	Department Chairperson

ACKNOWLEDGEMENTS

I would like to express my deepest appreciation to Dr. James F. Steffe, my major professor for providing the motive, the encouragement and sharing generously his experience and knowledge which have contributed in making this thesis a valuable experience for me.

Sincere appreciation is extended to Dr. Fred W. Bakker-Arkema and Dennis R. Heldman, members of the thesis committee for their valuable suggestions, constructive critism and sharing of their experiences through the course of the study.

My brother Awad-elseed is highly acknowledged for his support to me and to the family.

My thanks and appreciation is also extende to my wife, Anwar, for her support, understanding and encouragement. Special thanks is extended to Marnie Laurion for the typing of this thesis.

TABLE OF CONTENTS

																					Page
List	of	Table	s.	•			•	•	•	•	•	•	•	•	•	•	•	•	•	•	iv
List	of	Figur	es	•	•		•	•	•	•	•	•	•	•	•	•	•	•	•	•	v
List	of	Symbo	ls	•	•	•	•	•	•	•	•	•	•	•	•	•	•	•	•	•	vii
Char	oter	S																			
1.	INT	RODUCT	ION	•	• •		•	•	•	•	•	•		•	•	•	•	•	•	•	1
	1.1	Gene	ral	Rer	naı	ks	•	•	•	•	•	•	•	•	•	•	•	•	•	•	1
	1.2	Obje	cti	ves		•	•	•	•	•	•	•	•	•	•	•	•	•	•	•	2
2.	LITI	ERATUR	E R	EVII	EW	•	•	•		•	•	•	•	•	•	•	•	•	•	•	3
	2.1	Rheo	log	ica	LN	od	els	5	•	•	•	•	•	•	•	•	•	•		•	3
		2.1.	1 1	New	or	nia	n E	lu	iid	ls	•	•	•	•	•	•	•	•	•	•	3
		2.1.	2	Non-	-Ne	wt	on i	ian	F	'lu	id	s	•	•	•	•	•	•	•	•	3
			2.1	.2.	L	Ti									n-		•			•	4
			2.1	.2.2	2	Ti									•	•	•	•	•	•	7
				2.:	1.2	2.2	. 1	T	'hi	.xo	tr	op	oic	F	'1ບ	id	ls			•	7
				2.:	1.2	2.2	. 2	R	the	op	ec	ti	C	Fl	ui	ds	;	•		•	7
	2.2	Visc	ome	ter	5 .		•	•	•		•	•	•	•	•	•	•			•	9
		2.2.	1 1	Rota	ati	ion	al	۷i	sc	om:	et	er	•				•			•	10
			2.2	.1.	L	Co-	-ax	αia	1	Су	li	nd	ler	v	'is	cc	me	te	r	•	10
			2.2	.1.2	2	Si	ng]	le	Сy	'li	nd	er	. v	'is	cc	me	te	r	•	•	12
			2.2	.1.3	3	Co	ne	an	d	Pl	at	e	۷i	sc	on	et	er	•	•	•	13
			2.2	.1.4	Į.	Mi	xeı	. v	'is	sco	me	te	r	•				•	•	•	14
		2.2.	2 '	Tube	•	/is	con	net	er	•	•	•	•	•			•			•	18
3.	THE	ORETIC	AL (CONS	SII	DER.	AT I	ON	is	FC	R	HE	RS	СН	ŒL	E	UL	KL	.EY		
	FLU	IDS .	• •	•	• •	•	•	•	•	•	•	•	•	•	•	•	•	•	•	•	20
	3.1	Flow	Ra	te 1	Equ	ıat	ior	1 f	or	· 1	'ub	e	F1	OW	7	•			•		20

	3.2	Laminar-Transitional Flow Criterion .	•	•	•	24
4.	SENS	ITIVITY ANALYSIS	•	•	•	27
	4.1	Root Sum Square Error Model	•	•	•	27
	4.2	Derivatives of the Flow Model	•	•	•	28
	4.3	Verification of the Derivatives	•	•	•	30
	4.4	Sensitivity Analysis Calculations	•	•	•	33
	4.5	Laminar Flow Calculations	•	•	•	34
5.	RESU	LTS AND DISCUSSION	•	•	•	37
	5.1	Pressure Drop and Tube Geometry	•	•	•	37
	5.2	Effect of the Yield Stress	•	•	•	39
	5.3	Effect of the Consistency Coefficient	•	•	•	45
	5.4	Effect of the Flow Behavior Index	•	•	•	45
6.	CONC	LUSIONS	•	•	•	52
7	DEFE	DENCES				54

LIST OF TABLES

Table		F	age
1	Comparison between the analytical and numerical differentiation of flow rate with respect to the yield stress	•	32
2	Comparison between the analytical and numerical differentiation of flow rate with respect to flow behavior index	•	32

LIST OF FIGURES

Figure	<u> </u>	Page
1.	Relationship between shear stress and shear rate for different fluids not displaying time dependent behavior	6
2.	Flow curves for thixotropic and rheopectic fluids	8
3.	Schematic diagram of a co-axial cylinder viscometer	11
4.	Schematic diagram of a cone and plate viscometer .	15
5.	Velocity profile for Herschel-Bulkley fluid	21
6.	Flow chart showing the calculation scheme to evaluate the critical Reynolds number	35
7.	Critical Reynolds number as a function of the Hedstrom number and the flow behavior index	36
8.	Contour plot of an error of \pm 4.1% in flow rate which results from different values of pressure drop for K = 5.3 Pa·s ⁿ , Δ n = \pm 0.0001, Δ K = \pm 1.0% and Δ τ _y = \pm 0.5%	38
9.	Contour plot of an error of \pm 4.1% in flow rate which results from different values of pipe diameter for $K = 5.3 \text{ Pa} \cdot \text{s}^{\text{n}}$, $\Delta n = \pm 0.0001$, $\Delta K = \pm 1.0\%$ and $\Delta \tau = 0.5\%$	=
10.	Contour plot of an error of \pm 4.1% in flow rate which results from different values of pipe length for K = 5.3 Pa·s ⁿ , Δ n \pm 0.0001, Δ K = \pm 1.0% and Δ τ \pm 0.5%	= 41
11.	Percentage error in flow rate as a function of the yield stress, and flow behavior index for K = 5.3 Pa·s ⁿ , Δn = ± 0.0001, ΔK = ± 1.0% and $\Delta \tau_{Y}$ = ± 0.5%	42
12.	Percentage error in flow rate as a function of the yield stress and flow behavior index for K = 5.3 Pa·s ⁿ , $\Delta n = \pm$ 0.0001, $\Delta K = \pm$ 1.0% and $\Delta \tau_y = \pm$ 1.0%	43
13.	Percentage error in flow rate as a function of the yield stress and flow behavior index for K = 5.3 Pa·s ⁿ , $\Delta n = \pm 0.0001$, $\Delta K = \pm 1.0$ % and $\Delta \tau_y = \pm 3.0$ %	44
14.	Percentage error in flow rate as a function of the consistency coefficient and flow behavior index for τ = 7.67 Pa, Δn = \pm 0.0001, ΔK = \pm 0.5% and $\Delta \tau_y$ = $\frac{Y}{2}$ 1.0%	46

15.	Percentage error in flow rate as a function of the consistency coefficient and flow behavior index for τ_{y} = 7.67 Pa, Δn = \pm 0.0001, ΔK = \pm 1.0% and $\Delta \tau_{y}$ = \pm 1.0%	•	47
16.	Percentage error in flow rate as a function of the consistency coefficient and flow behavior index for τ_y = 7.67 Pa, Δn = \pm 0.0001, ΔK = \pm 3.0% and $\Delta \tau_y$ = \pm 1.0%	•	48
17.	Percentage error in flow rate as a function of the yield stress and flow behavior index for K = $5 \cdot 3$ Pa·s ⁿ , $\Delta n = \pm 0.001$, $\Delta K = \pm 1.0$ % and $\Delta \tau_y = \pm 1.0$ %	•	50
18.	Percentage error in flow rate as a function of the yield stress and flow behavior index for $K = 5.3$ Pa·s ⁿ . $An = + 0.01$. $AK = + 1.0$ % and $AT = + 1.0$ %.		51

LIST OF SYMBOLS

= dimensionless parameter defined by Eq. (38) Α В = constant defined by Eq. (16) C = constant defined by Eq. (18) D = tube diameter, m = fluid height, m h = Hedstrom number defined by Eq. (41) = constant defined by Eq. (17) k = consistency coefficient, Pa·sⁿ K = constant defined by Eq. (5) K K₁ = constant defined by Eq. (5) L = tube length, m = constant defined by Eq. (6) M = torque, N·m = flow behavior index = revolution per second N = power, N·m·s⁻¹ P = power number = volumetric flow rate, m³·s⁻¹ 0 = radius of the plug flow, m R = radius of the cone, m = radius of the bob, m Rh Re = Reynolds number Re' = rotational Reynolds number = critical Reynolds number $R_{\mathbf{w}}$ = radius of the tube, m

```
R<sub>2</sub>
       = radius defined by Eq. (10), m
       = velocity defined by Eq. (26), m \cdot s^{-1}
u
       = velocity defined by Eq. (28), m \cdot s^{-1}
       = average velocity defined by Eq. (37), m \cdot s^{-1}
ū
Ϋ́
       = shear rate, s<sup>-1</sup>
       = apparent shear rate defined by Eq. (17), s^{-1}
       = error in consistency coefficient, Pa·s<sup>n</sup>
\Delta K
       = error in flow behavior index
Δn
      = pressure drop, Pa
ΔΡ
      = error in flow rate, m^3 \cdot s^{-1}
ΔQ
\Delta \tau_{\mathbf{v}} = error in yield stress, Pa
       = plastic viscosity, Pa·s
       = viscosity, Pa·s
\xi_0 = \tau_{\mathbf{v}}/\tau_{\mathbf{w}}
       = fluid density, kg \cdot m^{-3}
       = dimensionless parameter defined by Eq. (35)
       = shear stress, Pa
^{\tau}b
       = shear stress at the bob, Pa
       = shear stress at the wall, Pa
τω
       = yield stress, Pa
\tau_{\mathbf{v}}
       = angle between cone and plate, rad
       = angular velocity, rad·s<sup>-1</sup>
```

1. INTRODUCTION

1.1 General Remarks

Rheological properties of fluid foods have many applications, including quality control (Rao et al., 1975) and design of fluid handling systems (Odigboh and Mohsenin, 1974; Boger and Tiu, 1975). In addition they are also essential for estimating heating rates (Sarvacos and Moyer, 1967), estimating overall heat transfer coefficients for evaporators (Harper, 1960) and correlation with sensory data (Dickie and Kokini, 1983).

Estimation of the rheological parameters is usually based on fitting viscometric data to rheological models. The accuracy achieved depends on how well the design of the viscometer satisfies the assumptions associated with the theoretical development. Poor understanding of the rheological techniques for non-Newtonian fluids can result in large errors. Rao et al. (1975) showed that errors of 20-50% on shear rate calculations can occur if Newtonian approximations are employed. This error will propogate and affect the estimation of the rheological parameters.

The idea for this investigation came from observations of the discrepancies among the published rheological data for the same products (Steffe et al. 1983). The work to be presented here will lead to a better understanding of tube flow phenomenon. It may lead to flow rate control based on pressure drop and be useful in the development of on-line viscometers for non-Newtonian fluids.

1.2 Objectives

The specific objectives of this investigation are:

- 1. To derive, then verify, published equations giving flow rate as a function of rheological parameters and pipe size for Herschel-Bulkley fluids.
- 2. To determine, from existing literature, the best technique for establishing laminar flow criterion in tube flow.
- 3. To develop the equations describing the sensitivity of flow rate to the flow behavior index, the consistancy coefficient and the yield stress.
- 4. To investigate the influence of the following in generating error in the calculated flow rate:
 - precision and magnitude of the flow behavior index;
 - precision and magnitude of the consistency coefficient;
 - precision and magnitude of the yield stress;
 - magnitude of pipe length, pipe diameter and pressure drop.

2. LITERATURE REVIEW

This section is devoted to a brief overview of the most common rheological models, and some of the viscometers used for measuring rheological properties.

2.1 Rheological Models

2.1.1 Newtonian Fluids

Newtonian fluids are those fluids having a linear relationship between shear stress and shear rate given by

$$\tau = \mu \dot{\gamma} \tag{1}$$

where

 τ = shear stress, Pa

u = viscosity. Pa·s

 \dot{Y} = shear rate, s⁻¹

This type of behavior may be observed with some juices, milk, oils and some other products. For Newtonian fluids, a single measurement can give satisfactory results in determining the viscosity.

2.1.2 Non-Newtonian Fluids

Non-Newtonian fluids are those for which the relation between shear stress and shear rate is not linear. These types of fluids can be divided into three broad groups:

- a. Time-independent fluids. These are fluids for which the shear stress does not change with time at a given shear rate.
- b. Time-dependent fluids. These are fluids for which the shear stress, at a constant shear rate, changes with time.

c. Viscoelastic fluids. These are fluids showing elastic recovery on removal of a deforming shear stress. Such materials posses properties of both a viscous fluid and an elastic solid. Viscoelastic fluids have a tendency to expand at the discharge end of the tube. This phenomenon known as die swell, is important for extruded foods. Viscoelastic fluids are characterized, in addition to the shear stress and shear rate deformation, by the normal stresses which involve complex mathematical models.

2.1.2.1 Time Independent Non-Newtonian Fluids

The flow behavior of fluids in this category has commonly been described by empirical models. In this review, the emphasis is on the most common models that are used to describe flow behavior of fluid foods. The power law model was found to describe a large spectrum of food material, according to a recent review by Steffe et al (1983). It is described as

$$\tau = K_{\gamma}^{*n}$$
 (2)

where

 $K = consistency index, Pa·s^n$

n = flow behavior index

When the value of n < 1, the fluid is known as pseudoplastic, which is the case with the majority of fluid foods. When the value of n > 1 the fluid is known as dilatant, a condition which is very rare with food products.

Figure (1) shows the shear stress versus shear rate for both fluid types.

Some food products possess a yield stress which must be overcome before flow can commence. A popular and generalized model which incorporates a yield stress was proposed by Herschel and Bulkley (1929) as

$$\tau = K_{\gamma}^{\bullet n} + \tau_{y}$$
 (3)

where

 τ_{v} = yield stress, Pa

Another model with yield stress and a direct relation between shear stress and shear rate, is known as the Bingham plastic model. This model was found to describe the flow behavior of food products such as casava starch (Odigboh, 1975) and is expressed by

$$\tau = \tau_{\mathbf{y}} + \zeta \dot{\gamma} \tag{4}$$

where

 ζ = plastic viscosity, Pa·s

The Casson model, developed for paint, was also found to have many applications with food products (Charm, 1962; Rao, 1981). It was adopted by the chocolate industry as the official model for describing the flow behavior of chocolate (Rao, 1977) and is given as

$$\tau^{1/2} = K_0 + K_1 \dot{\gamma}^{1/2}$$
 (5)

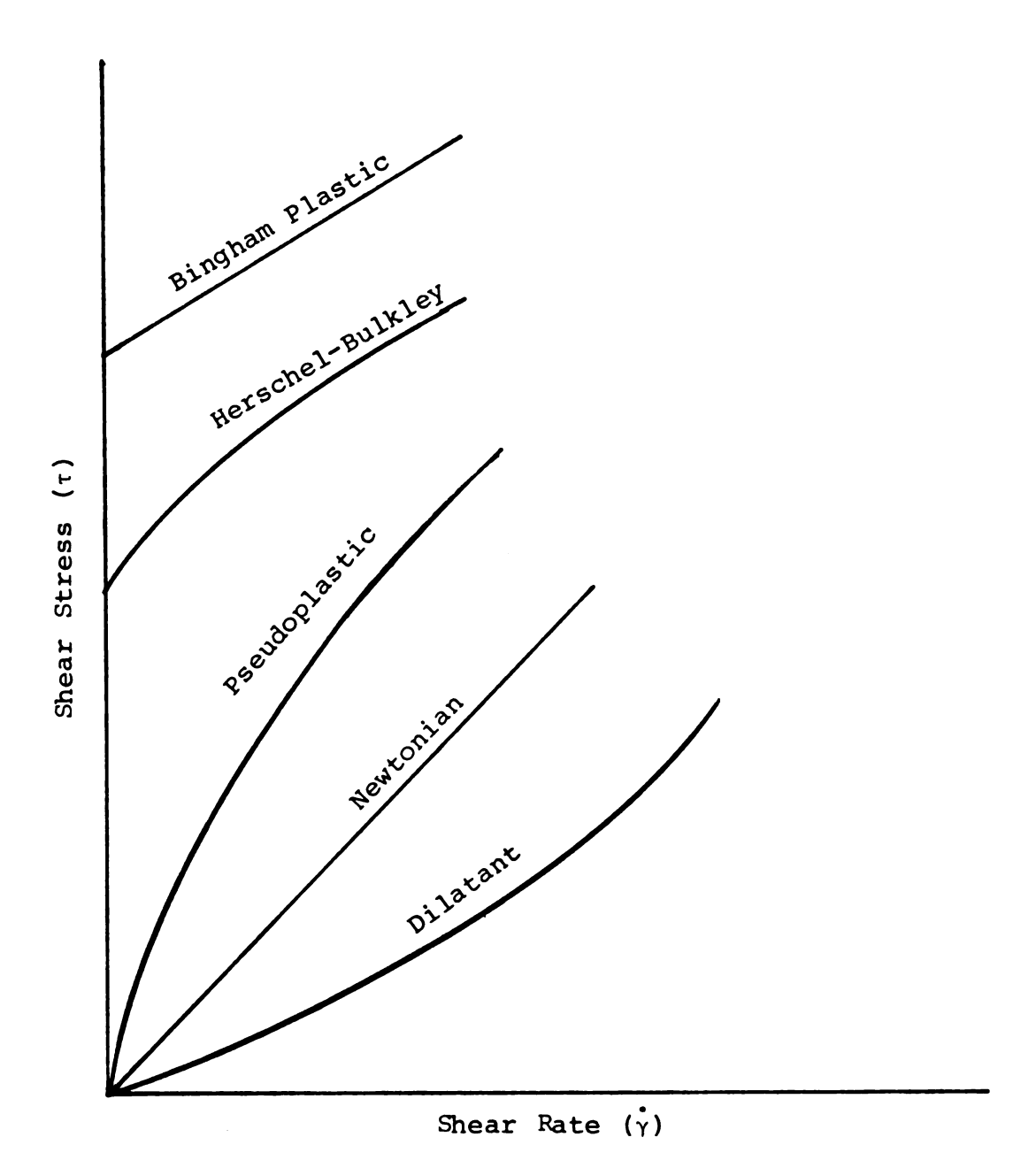


Figure 1. Relationship between shear stress and shear rate for different fluids not displaying time dependent behavior.

where

 ${\rm K_O}$ and ${\rm K_1}$ are constants. Mizrahi and Berk (1972) modified the Casson model to:

$$\tau^{1/2} = K_0 + K_{\gamma}^{*m} \tag{6}$$

where

m = constant.

This model was used successfully to fit orange juice data (Mizrahi and Berk, 1972).

2.1.2.2 Time-Dependent Non-Newtonian Fluids

These materials are usually divided into two major groups, thixotropic and rheopectic, depending on whether their shear stress decreases or increases with time, at a constant shear rate.

2.1.2.2.1 Thixotropic Fluids

Thixotropic fluids exhibit reversible decreases in shear stress, with time at constant temperature and shear rate. This phenomenon is explained by structural breakdown due to shearing (Green, 1949). If the shear stress is increased at steady rate and then decreased at steady rate, a hysteresis loop will be obtained (Figure 2). Irreversible breakdown due to mechanical degradation is known as rheomalaxis.

2.1.2.2.2 Rheopectic Fluids

These fluids are rare in occurrence and exhibit a

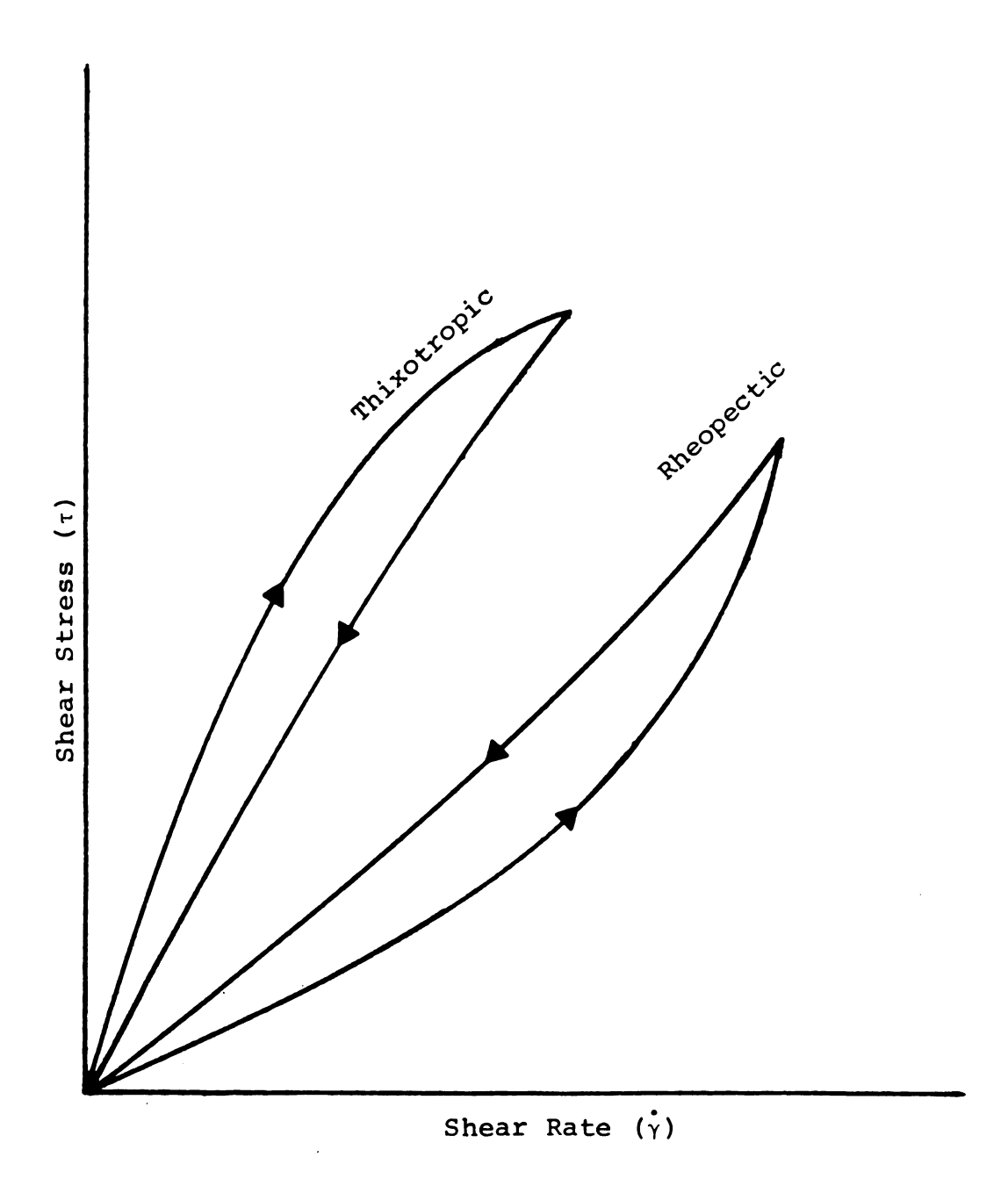


Figure 2. Flow curves for thixotropic and rheopectic fluids.

reversible increase in shear stress with time, at constant shear rate and temperature. These fluids also have a tendency to produce a loop if the shear stress is increased and then decreased at steady rate (Figure 2).

Green (1949) discussed a semi-quantitative approach to determine time-dependent changes in a co-axial cylinder viscometer. Measurement of the hysteresis loop between 'up' and 'down' curves is obtained, first by increasing the shear rate from a minimum to a maximum value using a predetermined incremental time step, then by decreasing it by the same step down to a minimum shear rate. The resulting loop will be indication of the thixotropy or rheopexy of the material. A larger hysteresis area implies that the fluid is more time-dependent and vice versa. Van Wazer et al. (1963) suggested a method of determining shear stress decay or built up as a function of time at one or more constant shear rates.

2.2 Viscometers

Viscometers are instruments used for the measurement of rheological parameters. A great number and diversity are available on the market, ranging from very simple and cheap, to sophisticated and expensive. The designs of these viscometers are based on various theoretical approaches which have different assumptions associated with them. The commonly used viscometers fall into two broad groups:

- a. rotational viscometers
- b. tube type viscometers

2.2.1 Rotational Viscometer

The main assumptions associated with this group are:

- a. flow is laminar,
- b. steady state,
- c. no end effect,
- d. isothermal flow,
- e. no slip at the wall,
- f. the fluid is homogeneous and incompressible.

2.2.1.1. Co-axial Cylinder Viscometer

Figure 3 shows the arrangement of this viscometer which consists of a bob of radius $R_{\rm b}$ that rotates on a cup of radius $R_{\rm c}$. The annulus of the cup should be kept to the minimum possible gap to satisfy some of the assumptions, mainly laminar flow. End effects can be minimized by maintaining a hollow cavity at the bottom of the bob, with the edge recessed, so as to trap air in this cavity and provide air-solid interface which has less drag compared to the liquid solid interface. The shear stress at the bob is given by

$$\tau_{\mathbf{b}} = \frac{\mathbf{M}}{2\pi R_{\mathbf{b}}^2 \mathbf{h}} \tag{7}$$

where

 τ_{h} = shear stress at the bob, Pa

M = torque, N·m

h = height of the fluid, m

 $R_h = radius of the bob, m$

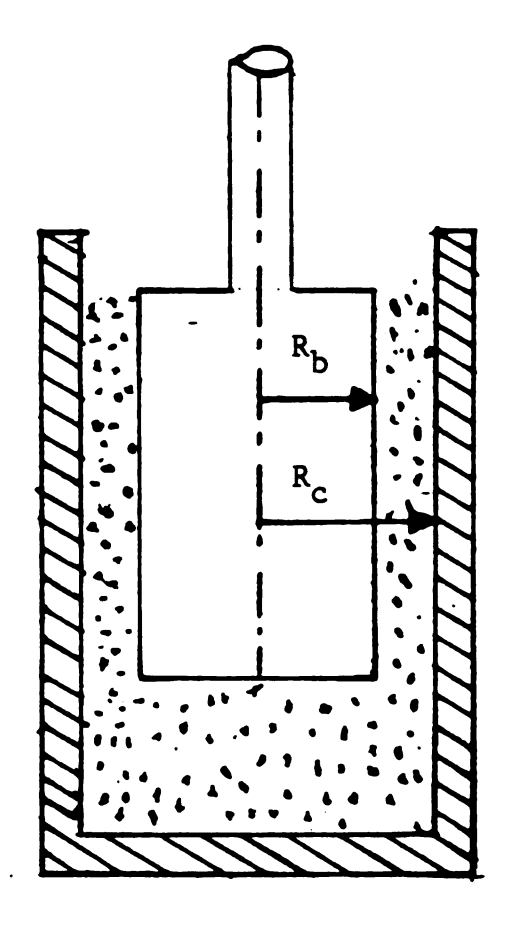


Figure 3. Schematic diagram of a co-axial cylinder viscometer.

A general expression for the shear rate at the bob was suggested by Kriger (1968) as

$$\tau_{b} = \frac{2\Omega}{S} \left[\frac{R_{c}^{2/S}}{R_{c}^{2/S} - R_{b}^{2/S}} \right] \left[1 + S^{2}S'f \left(\frac{2}{S} \ln \frac{R_{c}}{R_{b}} \right) \right]$$
(8)

where

$$\frac{1}{S} = \frac{d(\ln \Omega)}{d(\ln \tau_b)}$$

$$S' = \frac{d(1/S)}{d(\ln \tau_b)}$$

$$f(t) = \frac{t(e^t(t-2) + t + 2)}{2(e^t - 1)^2}$$

 Ω = angular velocity, rad/s

2.2.1.2. Single Cylinder Viscometer

Charm (1963) derived a relation between the rheological parameters of fluid with yield stress and the physical parameters of the viscometer system given by

$$2\pi N \left(\frac{K}{\tau_y}\right)^{1/n} = \int_{R_1}^{R_2} \left(1 - \frac{M}{2\pi h R^2 \tau_y}\right)^{1/n} \frac{dR}{R}$$
 (9)

where

M = torque, N·m

 R_1 = radius of the cylindrical spindle, m

R₂ = distance from the center of the spindle to where the shear stress just equals the yield stress, m

h = height of the fluid, m

N = revolution per second

Using Equation (7), R2 can be expressed as

$$R_2 = \frac{M}{2\pi h \tau_Y} \tag{10}$$

The solution to Equation (9) is difficult to perform analytically. Charm has suggested a graphical solution, after determination of the yield stress.

For the power law fluid the relation is

$$2\pi N = \frac{n}{2} \left(\left(\frac{M}{2\pi hK} \right)^{1/n} \right) \left(\frac{1}{R_h^{2/n}} \right)$$
 (11)

where

 R_h = radius of the spindle, m

Using Equation (11), the rheological parameters can easily be determined; by plotting N versus M/n on double logarithmic paper, the slope will be 1/n. Then, K can be found by substitution using Equation (11).

2.2.1.3 Cone and Plate Viscometer

The cone and plate is a rotational viscometer used for direct measurement of shear stress and shear rate. It is also used with some modification to measure the normal stresses for viscoelastic fluids. The viscometer consists of an obtuse angle cone and a flat plate. The apex of the cone just touches the plate and the fluid fills the narrow

gap formed by the cone and the plate. The angle between the cone and the plate is usually made very small to ensure a uniform rate of shear (Figure 4). The expression for the shear rate and the shear stress is given by

$$\dot{\dot{\gamma}} = \frac{\Omega}{\tan \psi} \tag{12}$$

$$\tau = \frac{3M}{2\pi R^3} \tag{13}$$

where.

 $M = torque, N \cdot m$

 Ω = angular velocity, rad/s

 ψ = angle between cone and plate, rad

R = radius of the cone, m

2.2.1.4 Mixer Viscometer

Some of the specific assumptions of this viscometer are:

- a. the rotational Reynolds number must be in the laminar flow region (less than 10).
- b. the power law parameters for the standard fluid must be valid over the range of shear rates that would be exerted by the mixer.
- c. the standard and the unknown fluid must not be viscoelastic.

The power input to a mixing vessel, derived from

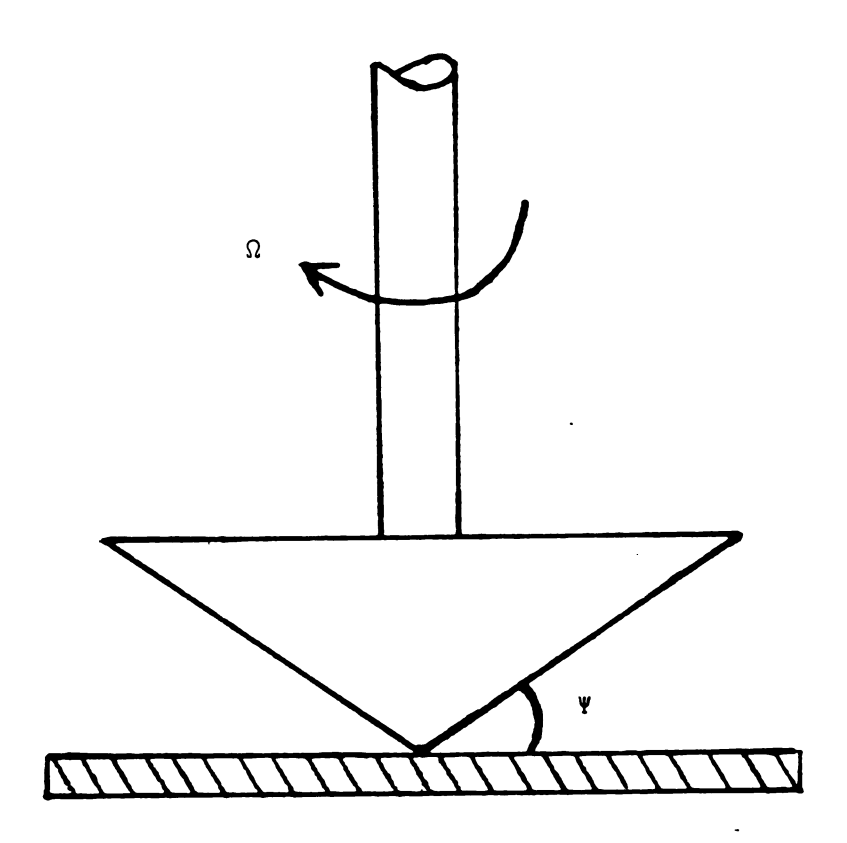


Figure 4. Schematic diagram of a cone and plate viscometer.

dimensional analysis, is a function of the power number and mixing Reynolds number given as

$$P_{o} = P/(d^{5}N^{3}\rho) \tag{14}$$

$$Re' = d^2N\rho/\mu \tag{15}$$

where

 $P = power, N \cdot m/s$

P = power number

d = diameter of the impler, m

N = revolution per second

 ρ = density of the fluid, kg/m³

μ = viscosity of the fluid, Pa·s

Re' = rotational Reynolds number

For laminar conditions the power curve is given by

$$P_{o} = \frac{B}{Re^{T}}$$
 (16)

where

B = constant dependent on the impeller geometry.

Mentzer and Otto (1957) suggested a relation for the average shear rate, to be used for calculating the apparent viscosity which is then to be used to calculate the Reynold number, as

$$\dot{\gamma}_a = kN \tag{17}$$

where

 $\dot{\gamma}$ = average shear rate, s^{-1}

k = constant depending on the impeller geometry

N = rotational speed revolution per second

The shear stress at the impeller is given by:

$$\tau = CM \tag{18}$$

where

C = constant

 $M = torque, N \cdot m$

To determine the flow behavior index (n_x) for the power law fluid (x), a logarithmic plot of M and N should be made for which the slope will be the flow behavior index. For determining the consistency coefficient K_x , a standard fluid (Y) of approximately the same flow behavior index (n_y) is used.

Using Equations (17) and (18) in Equation (2) we get,

$$\frac{M_{\mathbf{X}}}{M_{\mathbf{Y}}} = \frac{\tau_{\mathbf{X}}}{\tau_{\mathbf{Y}}} = \frac{K_{\mathbf{X}}^{\mathbf{N}} K_{\mathbf{X}}^{\mathbf{N}} K_{\mathbf{X}}^{\mathbf{N}}}{K_{\mathbf{Y}}^{\mathbf{N}} Y_{\mathbf{K}}^{\mathbf{N}} Y}$$
(19)

If $n_x = n_v$ equation (19) can be reduced to

$$\frac{K_{X}}{K_{Y}} = \frac{M_{X}}{M_{Y}} \tag{20}$$

From Equation (20), K_x can be found from the knowledge of K_y and the induced torque for both fluids at a specific speed. Mixer viscometer can be used to obtain the rheological parameters when particle sizes in the fluids are relatively large (too large for co-axial cylinder viscometers) or when the fluid particles have a tendency to settle causing the material to become in homogeneous. Bongenaar et al. (1973) and Rao (1975) used mixer viscometry successfully to find the rheological parameters of the power law fluids.

2.2.2 Tube Viscometer

The assumptions associated with this type of viscometer are

- a. flow is laminar,
- b. flow is steady,
- c. no slip at the wall,
- d. isothermal flow,
- e. no end effects,
- f. the fluid is homogeneous and incompressible.

The shear stress at the wall for tube viscometer is given by

$$\tau_{W} = \frac{\Delta P \cdot D}{4L} \tag{21}$$

where

 ΔP = pressure drop, Pa

D = tube diameter, m

L = tube length, m

Rabinowitsch (1929) developed an expression for the rate of shear for time-independent fluids which is entirely independent of the fluid properties. The complete development of this equation was also presented in a paper by Mooney (1931). Their final expression is

$$\dot{\gamma} = \frac{3Q}{\pi R^3} + \tau_{w} \frac{d(Q/\pi R^3)}{d(\tau_{w})}$$
 (22)

where

 $Q = flow rate, m^3/s$

From equation (22) the relation for the true shear rate for the power law fluid can be obtained as

$$\dot{\gamma} = \left(\frac{32Q}{\pi D^3}\right) \left(\frac{3n+1}{4n}\right) \tag{23}$$

Similar expressions for Newtonian and Bingham plastic fluids are also available.

3. THEORETICAL CONSIDERATIONS FOR HERSCHEL-BULKLEY FLUIDS

In this section efforts have been made to derive a generalized flow rate equation for fluids obeying the Herschel-Bulkley (H-B) model, to be used later in the analysis. One of the main assumptions associated with the use of the flow rate equation, is that the flow is laminar. A criterion for laminar flow as developed by Hanks (1974) will also be presented.

3.1. Flow Rate Equation For Tube Flow

In the derivation of the flow rate equation for a H-B fluid, the assumptions stated for the tube viscomer will also apply. Consider a tube of length L and radius R, with the pressure drop between two points (1 and 2) as ΔP , and the radius of the plug flow region being r_o (Figure 5). When pressure is applied to the core of the fluid, the fluid moves with two distinct velocity profiles. For the region from the center to where the shear stress equals the yield stress, the fluid moves with constant velocity. For the region where the yield stress is exceeded, the fluid has a velocity profile which is a function of the radial distance from the center line. The shear stress at the wall is given by Equation (21).

Applying balanced force on the core of the fluid between points 1 and 2 shown on Figure 1 yields

$$\Delta P \pi r^2 = 2 \pi r L \tau \tag{24}$$

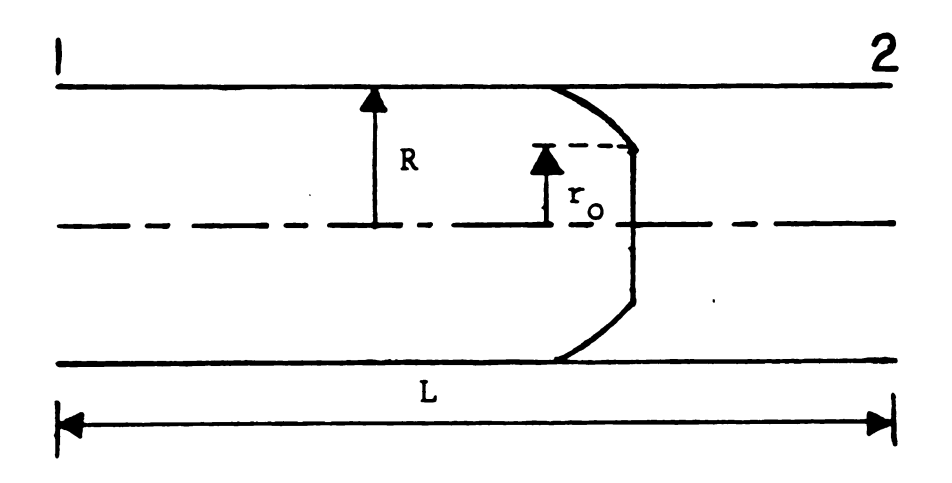


Figure 5. Velocity profile for Herschel-Bulkley fluid.

Substituting for τ from the H-B equation (Equation (3)), we get

$$\Delta P \pi r^2 = \left[-K \left(\frac{du}{dr} \right)^n + \tau_y \right] 2 \pi r L \qquad (25a)$$

Equation (25) can be rearranged as

$$-\frac{\mathrm{d}\mathbf{u}}{\mathrm{d}\mathbf{r}} = \frac{1}{\kappa^{1/n}} \left[\frac{\Delta P \cdot \mathbf{r}}{2L} - \tau_{\mathbf{y}} \right]^{1/n} \tag{25b}$$

For no slip conditions, equation (25b) can be integrated over the tube giving

$$-\int_{u}^{o} du = \frac{1}{\kappa^{1/n}} \int_{r}^{R_{w}} \left[\frac{\Delta Pr}{2L} - \tau_{y} \right]^{1/n} dr \qquad (25c)$$

After integration and substitution of the limits, the velocity becomes

$$u = \frac{2L}{\Delta P K^{1/n}} \left[\frac{\left(\frac{\Delta P R_{W}}{2L} - \tau_{y}\right)^{((1/n)+1)} - \left(\frac{\Delta P \gamma}{2L} - \tau_{y}\right)^{((1/n)+1)}}{((1/n)+1)} \right]$$
(26)

The plug radius, r_0 is given by

$$r_{o} = \frac{2\tau_{v}L}{\Lambda P}$$
 (27)

The velocity of the plug region u_{max} can be found by substituting r_o from Equation (27) into Equation (26) yielding

$$u_{\text{max}} = \frac{2L}{\Delta P K^{1/n}} \left(\left(\frac{\Delta P R_2}{2L} - \tau_{Y} \right)^{((1/n)+1)} \right) \left(\frac{1}{((1/n)+1)} \right)$$
 (28)

For the unplug region, the volumetric flow rate can be expressed by

$$Q_{1} = \int_{\mathbf{r}_{0}}^{\mathbf{R}_{\mathbf{W}}} u2\pi r dr \qquad (29)$$

$$Q_{1} = \frac{2\pi}{((1/n)+1)\left(\frac{\Delta P}{2L}\right)K^{1/n}} \left\{ \left(\frac{\left(\frac{\Delta PR_{2}}{2L} - \tau_{y}\right)^{((1/n)+1)}}{2} (R_{w}^{2} - \gamma_{o}^{2}) - \left(\frac{\Delta PR_{w}}{2L} - \tau_{y}\right)^{((1/n)+2)} (R_{w}^{2} - \gamma_{o}^{2}) - \left(\frac{\Delta PR_{w}}{2L} - \tau_{y}\right)^{((1/n)+2)} \left(\frac{\Delta PR_{w}}{2L} - \tau_{y}\right)^{((1/n)+2)} \left(\frac{\Delta PR_{w}}{2L} - \tau_{y}\right)^{((1/n)+2)} \right\}$$
(30a)

Substituting the value of r_o and introducing τ_w , Equation (30a) can be reduced to

$$Q_{1} = \frac{\pi R^{3} (\tau_{w} - \tau_{y})}{R^{1/n} \tau_{w}^{3}}$$

$$\left[\frac{((1/n)+1)((1/n)+2) \tau_{w}^{2} + 2((1/n)+1) \tau_{w} \tau_{y} - ((1/n)+1)((1/n)+4)}{((1/n)+1)((1/n)+2)((1/n)+3)}\right]$$
(30b)

For the plug region the flow rate is given by

$$Q_2 = \int_0^{r_0} u_{\text{max}} 2\pi r d\gamma$$

Substituting u_{max} and integrating yields

$$Q_{2} = \left(\frac{\pi R^{3} \left(\tau_{w} - \tau_{y}\right)^{((1/n)+1)}}{\pi^{1/n} \tau_{w}^{3}}\right) \left(\frac{\tau_{y}^{2}}{((1/n)+1)}\right)$$
(31)

The total volumetric flow rate Q is

$$Q = Q_1 + Q_2 \tag{32}$$

By substituting Equations (30b) and (31) into (32), with some algebraic manipulation, the result is

$$Q = \frac{\pi R^{3} (\tau_{w}^{-} \tau_{y}^{-})^{((1/n)+1)}}{\kappa^{1/n} \tau_{w}^{3}} \left[\frac{((1/n)+1)((1/n)+2) \tau_{w}^{2} + 2((1/n)+1) \tau_{w} \tau_{y}^{+} + 2 \tau_{y}^{2}}{((1/n)+1)((1/n)+2)((1/n)+3)} \right] (33)$$

Equation (33) is the same as that given by Nakayama et al. (1984).

3.2 Laminar-Transional flow Criterion

Numerous attempts have been made to develop an analytical criterion for the laminar-transional region for non-Newtonian fluids (Metzner and Reed, 1955; Ryan and Johnson, 1959; Hanks and Christiansen, 1962; Hanks, 1969; Hanks and Ricks, 1974). For all the methods developed, Hanks and Ricks (1974) seems to have succeeded in developing a most generalized approach which will be outlined in this section.

Hanks and Ricks (1974) developed a generalized relation for the Reynolds number that accounts for the yield stress given by the following series of equations:

$$Re = 8 \rho R_{w} \bar{u}^{(2-n)} \left[\left[\frac{n}{1+3n} \right]^{n} \right] \left[\frac{\sigma}{K} \right]$$
 (34)

where

$$\sigma = (1-\xi_0)^{1+n} \left[(1-\xi_0)^2 + 2 \xi_0 (1-\xi_0) \left(\frac{1+3n}{1+2n} \right) + \xi_0^2 \left(\frac{1+3n}{1+n} \right) \right]^n$$
 (35)

$$\xi_{o} = \frac{\tau_{y}}{\tau_{w}} \tag{36}$$

$$\bar{u} = \left(\left(\frac{A \tau_{w}}{K} \right)^{1/n} \right) R_{w}$$
 (37)

$$A = \sigma \left(\frac{n}{1+3n}\right)^n \tag{38}$$

 R_{w} = pipe radius, m

K, n, $\boldsymbol{\tau}_{\boldsymbol{y}}$ are parameters of the H-B fluid model.

From the use of the stability theory developed by Hanks (1969), Hanks and Ricks (1974) developed a relation for the critical Reynolds number given as

$$Re_{C} = \left[\frac{6464}{(1+3n)^{2}}\right] \left[\frac{(2+n)^{\frac{2+n}{1+n}} \sigma_{C}^{\frac{2}{n}}}{(1-\xi_{C})^{\frac{2+n}{n}}}\right]$$
(39)

where ξ_{oC} given by

$$\frac{\xi_{\circ C}}{(1-\xi_{\circ C})} \frac{((2/n)-1)}{((2/n)+1)} = \left(\frac{nH\rho}{3232}\right) \left(\frac{1}{2+n}\right)^{\frac{2+n}{1+n}}$$
(40)

and \mathbf{H}_{0} , the generalized Hedstrom number, is defined as

He =
$$\frac{D^2 \rho}{\tau_y} (\tau_y/K)^{2/n}$$
 (41)

 σ_c is given by Equation (35) with $\xi_o = \xi_{oc}$.

Based on the previous analysis Hanks generated a series of curves showing the influence of the Hedstrom number and the flow behavior index on the critical Reynolds number. It is interesting to note that Hanks and Ricks (1974) found an explanation (from previous experimental data for fluid with yield stress) for the trend of the critical Reynolds number at low values of flow behavior index (Hanks, 1962). Hanks and Ricks (1974) stated in this regards that, "The Metzner and Reed (1955) method of fitting a variable parameter power law to a non-Newtonian system having a low n value is risky since it ignores any yield values." Errors of several hundred percent were shown to occur when the Metzner and Reed (1955) method was used.

4. SENSITIVITY ANALYSIS

4.1. Root Sum Square Error Model

Consider a problem of computing Q, where Q is known function of n independent variables q_1 , q_2 , q_3 . . . q_n or

$$Q = f(q_1, q_2, q_3 - - - q_n)$$
 (42)

If the q values are measureable quantities, and they are in error by $\pm \Delta q_1$, $\pm \Delta q_2$, . . . $\pm \Delta q_n$ respectively, these errors result in error Q according to the following relation

$$Q \pm \Delta Q = f (q_1 \pm \Delta q_1, q_2 \pm \Delta q_2 - - - q_n \pm \Delta q_n)$$
 (43)

The right hand side of Equation (43) can be expanded in Taylor's Series as

$$f(q_1 \pm \Delta q_1, q_2 \pm \Delta q_2 - - - q_n \pm \Delta q_n) = f(q_1, q_2 - - - - q_n)$$

$$\pm \Delta q_1 \left(\frac{\partial f}{\partial q_1}\right) \pm \Delta q_2 \left(\frac{\partial f}{\partial q_2}\right) - - - \pm \Delta q_n \left(\frac{\partial f}{\partial q_n}\right) \pm \frac{1}{2} \left[(\Delta q_1)^2 \left(\frac{\partial^2 f}{\partial q_2^2}\right) \pm (\Delta q_2)^2\right]$$

$$\left(\frac{\partial^2 f}{\partial q_n^2}\right) - - - \pm (\Delta q_n)^2 \left(\frac{\partial^2 f}{\partial q_n^2}\right) \pm - - - -$$

$$(44)$$

If the values of $\triangle q$ are small quantities, then the higher order terms can be neglected giving

$$Q \pm \Delta Q = f(q_1, q_2, --- q_n) \pm \Delta q_1 \left(\frac{\partial f}{\partial q_1}\right) \pm \Delta q_2 \left(\frac{\partial f}{\partial q_2}\right) --- \pm \Delta q_n \left(\frac{\partial f}{\partial q_n}\right)$$
 (45)

Hence, from Equation (45)

$$\Delta Q = \Delta q \left(\frac{\partial f}{\partial q_1}\right) \pm \Delta q_2 \left(\frac{\partial f}{\partial q_2}\right) \pm - - - \Delta q_n \left(\frac{\partial f}{\partial q_n}\right)$$
 (46)

The expression for ΔQ holds for any kind of error (Scarborough, 1966). If we assume that the error made in measuring q_1, q_2, \ldots, q_n to be independent and completely random, then the maximum allowable error in Q can be given by the root sum square formula written by Scarborough (1966) as

$$\Delta Q = \sqrt{\left(\Delta q_1 - \frac{\partial f}{\partial q_1}\right)^2 + \left(\Delta q_2 - \frac{\partial f}{\partial q_2}\right)^2 + - - - \left(\Delta q_n - \frac{\partial f}{\partial q_n}\right)^2}$$
 (47)

Equation (47) is an indirect measurement of the maximum probable error of Q when the errors in the independent variable are known.

4.2. Derivatives of the Flow Model

The flow rate for a Herschel-Bulkley fluid is a function of the rheological parameters as well as pressure drop and tube geometry. In this analysis, the intent is to investigate the effect of the rheological parameters on flow rate calculations which can be achieved by considering the pressure drop and tube geometry to be constant; therefore, we can write flow rate as

$$Q = f(K, n, \tau_y)$$
 (48)

If we assume that the error made in measuring K, n and τ_y to be independent and completely random, then the maximum allowable error can be given by the root sum square formula

$$\Delta Q = \sqrt{\left(\frac{\partial Q}{\partial \mathbf{n}} \Delta \mathbf{n}\right)^2 + \left(\frac{\partial Q}{\partial K} \Delta K\right)^2 + \left(\frac{\partial Q}{\partial \tau_{\mathbf{y}}} \Delta \tau_{\mathbf{y}}\right)^2} \tag{49}$$

Equation (49) was used to investigate the effect of error in flow rate which results from measurement errors in the rheological parameter. First, the partial derivatives in Equation (49) were evaluated and found to be

$$\frac{\partial Q}{\partial n} = \frac{\pi R^3 \left(\tau_w - \tau_y\right) \left((1/n) + 1\right)}{R^{1/n}} \left\{ \frac{1}{n^2 \tau_w} \left(\frac{\ln R}{(1/n) + 3} + \frac{1}{(1/n) + 3} \right) - \ln \frac{\left(\tau_w - \tau_y\right)}{\left((1/n) + 3\right)} + \frac{2\tau_y}{\tau_w^2} \left(\frac{\ln R}{(1 + 5n + 6n^2)} + \frac{\frac{2}{n^3} + \frac{5}{n^2}}{\left(\frac{1}{n^2} + \frac{5}{n} + 6\right)^2} - \ln \frac{\left(\tau_w - \tau_y\right)}{(1 + 5n + 6n^2)} \right)$$

$$+ \frac{\tau_y^2}{\tau_w^3} \left(\frac{\ln R}{\left(\frac{1}{n} + 1\ln + 6n^2 + 6\right)} + \frac{\frac{3}{n^4} + \frac{12}{n^3} + \frac{11}{n^2}}{\left(\frac{1}{n^3} + \frac{6}{n^2} + \frac{11}{n} + 6\right)^2} \right)$$

$$(50)$$

$$\frac{\partial Q}{\partial K} = \left(\frac{\pi R^3 \left(\tau_W^{-\tau_V}\right)^{((1/n)+1)}}{n \tau_W^3 K^{((1/n)+1)}}\right) \left(\frac{\tau_W^2 \left((1/n)+1\right) \left((1/n)+2\right) + 2\tau_W^{-\tau_V} \left((1/n)+1\right) + 2\tau_V^2}{\left((1/n)+1\right) \left((1/n)+2\right) \left((1/n)+3\right)}\right)$$
(51)

and

$$\frac{\partial Q}{\partial \tau_{y}} = \left(\frac{\pi R^{3} (\tau_{w}^{-\tau_{y}})^{1/n}}{\tau_{w} K^{1/n}}\right) \left(2 \left(\frac{(\tau_{w}^{-\tau_{y}}) - ((1/n)+1) \tau_{y}}{\tau_{w} ((1/n)+2) ((1/n)+3)}\right) + \left(\frac{2 \tau_{y}^{-\tau_{y}} (\tau_{w}^{-\tau_{y}}) - ((1/n)+1) \tau_{y}^{2}}{\tau_{w}^{2} ((1/n)+1) ((1/n)+2) ((1/n)+3)}\right) - \left(\frac{((1/n)+1)}{((1/n)+3)}\right)\right)$$
(52)

Equations (50), (51) and (52) will be incorporated into Equation (49). These equations are not available in published literature.

4.3 Verification of the Derivatives

The partial derivatives of the independent variables presented in Section 4.2 are analytical expressions. Due to the complexity of the equations, it was necessary to check their accuracy, especially the derivatives with respect to yield stress and flow behavior index. This check was accomplished by comparing results to independent analytical solutions and numerical solutions.

The flow rate equation for the power law fluid is

$$Q = \frac{\pi R^3}{K^{1/n}} \left(\tau_{\mathbf{w}}^{1/n} \right) \left(\frac{n}{(3n+1)} \right)$$
 (53)

When Equation (53) is differentiated with respect to n, it yields

$$\frac{\partial Q}{\partial n} = \frac{\pi R^3}{K^{1/n}} \left(\frac{\ln K}{n^2 ((1/n) + 3)} + \frac{1}{n^2 ((1/n) + 3)^2} - \frac{\ln \tau_w}{n^2 ((1/n) + 3)} \right)$$
 (54)

When a value of zero yield stress is substituted into Equation (50), it reduces to Equation (54), indicating that Equation (50) is correct for the special case of the power law.

For checking the derivative with respect to the yield stress, consider the flow rate equation for Bingham plastic fluid, known as Buckingham equation given as

$$Q = \frac{\pi R^3 \tau_w}{4 \eta} \qquad [1 - \frac{4}{3} (\tau_y / \tau_w) + \frac{1}{3} (\tau_y / \tau_w)^4] \qquad (55)$$

The derivative with respect to the yield stress for Equation (55) is

$$\frac{\partial Q}{\partial \tau_{\mathbf{y}}} = \frac{\pi R^3}{3 \eta} \left[\left(\tau_{\mathbf{y}} / \tau_{\mathbf{w}} \right)^3 - 1 \right]$$
 (56)

With the substitution of n = 1 into Equation (52), the result is identical to Equation (56), showing Equation (52) to be correct for the special case of the Bingham plastic fluid. Similar results are found when considering a Newtonian fluid.

In addition to the method just outlined, a numerical technique employing Euler forward difference method is used for further checking. The values of pressure drop and tube dimension used are the same for both cases, with values typical to those used later for the analysis. The results are shown in Tables (1) and (2). It is clear that the analytical results are very close to the numerical results.

Table 1. Comparison between the analytical and numerical differentiation of flow rate with respect to the yield stress.

τy	2		10		
n	. 2	.5	.2	.5	
analytical	5.793x10 ⁻⁵	43.80×10 ⁻⁷	7.3162×10^{-7}	4.3198x10 ⁻⁷	
numerical	5.780x10 ⁻⁵	43.59x10 ⁻⁷	7.3137x10 ⁻⁷	4.3181x10 ⁻⁷	
% difference	0.224%	0.479%	0.031%	0.039%	

Table 2. Comparison between the analytical and numerical differentiation of flow rate with respect to flow behavior index.

n	. 2	• 5	.7
analytical	11.593×10 ⁻⁵	0.558x10 ⁻⁵	0.199×10 ⁻⁵
numerical	11.592x10 ⁻⁵	0.546×10 ⁻⁵	0.188×10^{-5}
% difference	0.0086%	2.150%	5.527%

This is further evidence supporting the reliability of the analytical solution. The small difference observed can be attributed to the limitations associated with the numerical solution technique. For the derivative with respect to the consistency coefficient, the exact value was obtained

4.4 Sensitivity Analysis Calculations

A Fortran computer program was written to perform all calculations. Two subroutines, from the main MSU computer system (subroutine C, Plot A and subroutine C, Plot B), were attached to the program to perform contour plotting of the flow rate error as a function of the independent variables under consideration. The subroutines have the capability of establishing the scale and the interval of the contour plot.

To perform the calculations, the values of the parameters, tube geometry, and pressure drop are inputed to the program. To investigate the influence of the effect of pressure drop (ΔP), tube length (L), and tube diameter (D), the following three values of each were used:

- ΔP: 8.0kPa, 10.0kPa, 12.0kPa
- L: 4.0m, 6.0m, 8.0m
- 0.0254m, 0.0381m, 0.0762m

A pressure drop of 8.0kPa, a length of 6(m) and diameter of 0.0381 (m) were used as fixed parameters to investigate the sensitivity of Q to the rheological parameters. These values were chosen because they are typical of what might be found in an actual fluid handling system.

The magnitude and precision level considered for the

rheological parameters are typical of fluid food products and summarized as follows:

- 1. $3.0 < K < 10.0 \text{ Pa·s}^n$ at ΔK , $\pm 0.5\%$, $\pm 1.0\%$ and $\pm 3\%$
- 2. $0.2 \le n \le 1.0$ at Δn , \pm 0.0001, \pm 0.001 and \pm 0.01
- 3. $3.0 \le \tau_y \le 10.0 \text{ Pa}$ at $\Delta \tau_y$, $\pm 0.5\% \pm 1.0\%$ and $\pm 3.0\%$

4.5 Laminar Flow Calculations

The condition of laminar flow is the one generally found with non-Newtonian fluid food products and the analysis of the current work is based on flow of this type. A computer program based on Hanks and Ricks (1974) method, was written to calculate the flow and the critical Reynolds numbers. The computer program utilized the equations presented in Section 3.2. An iterative procedures was used to calculate the parameter $\xi_{\rm oc}$. Figure (6) shows the flow chart for calculating the critical Reynolds number. Some of the curves generated from the computer program are shown in Figure (7). These curves are the same as those presented in Hanks and Ricks (1974) paper.

The calculation of the flow Reynolds number, starts by calculating ξ_0 from Equation (36) which is used in Equation (35) to calculate σ . Equations (35) and (38) were then evaluated respectively, to solve for \bar{u} (Equation 37) which is to be used with the rheological parameters, pipe radius, and fluid density to evaluate the Reynolds number from Equation (34).

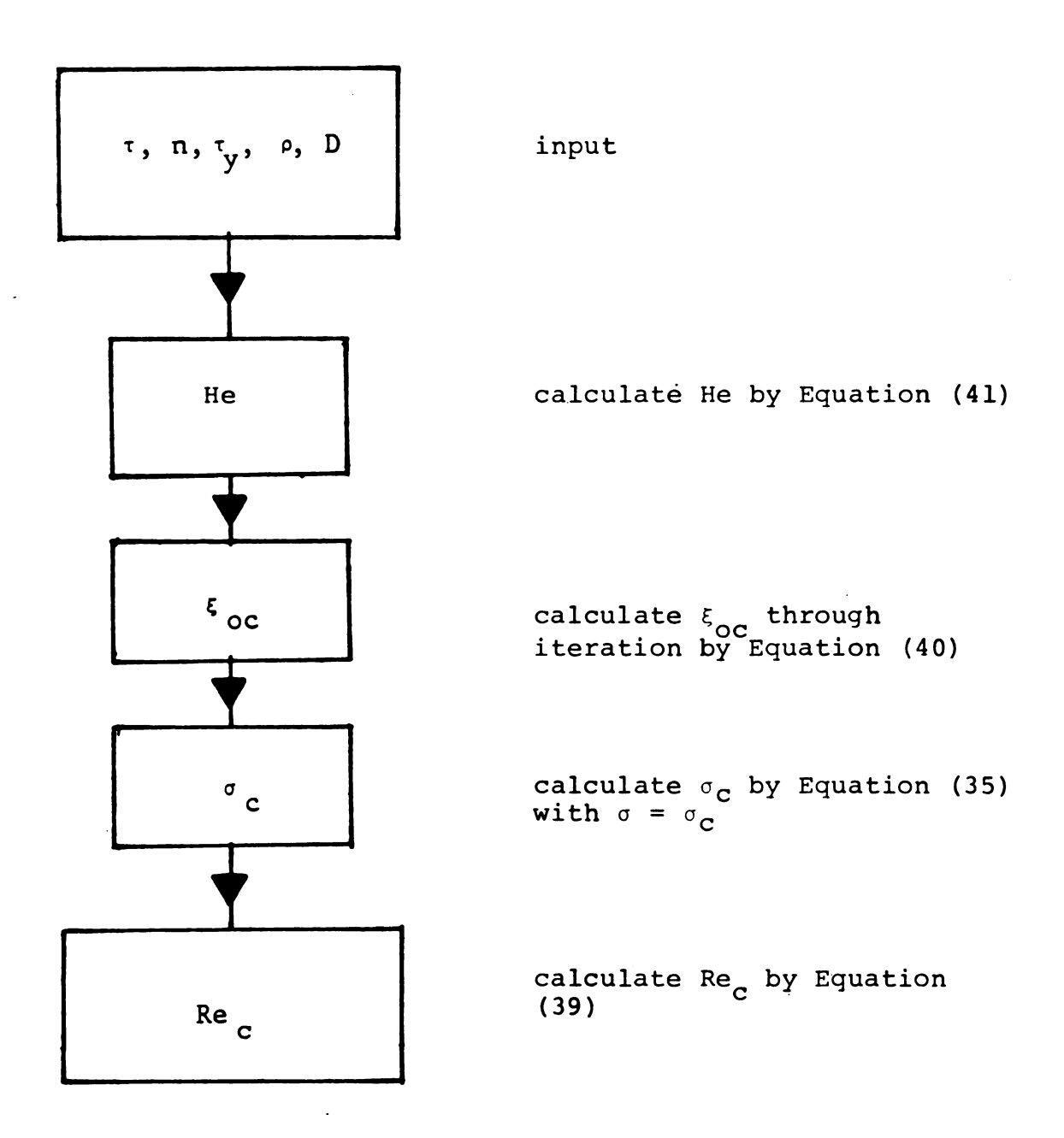
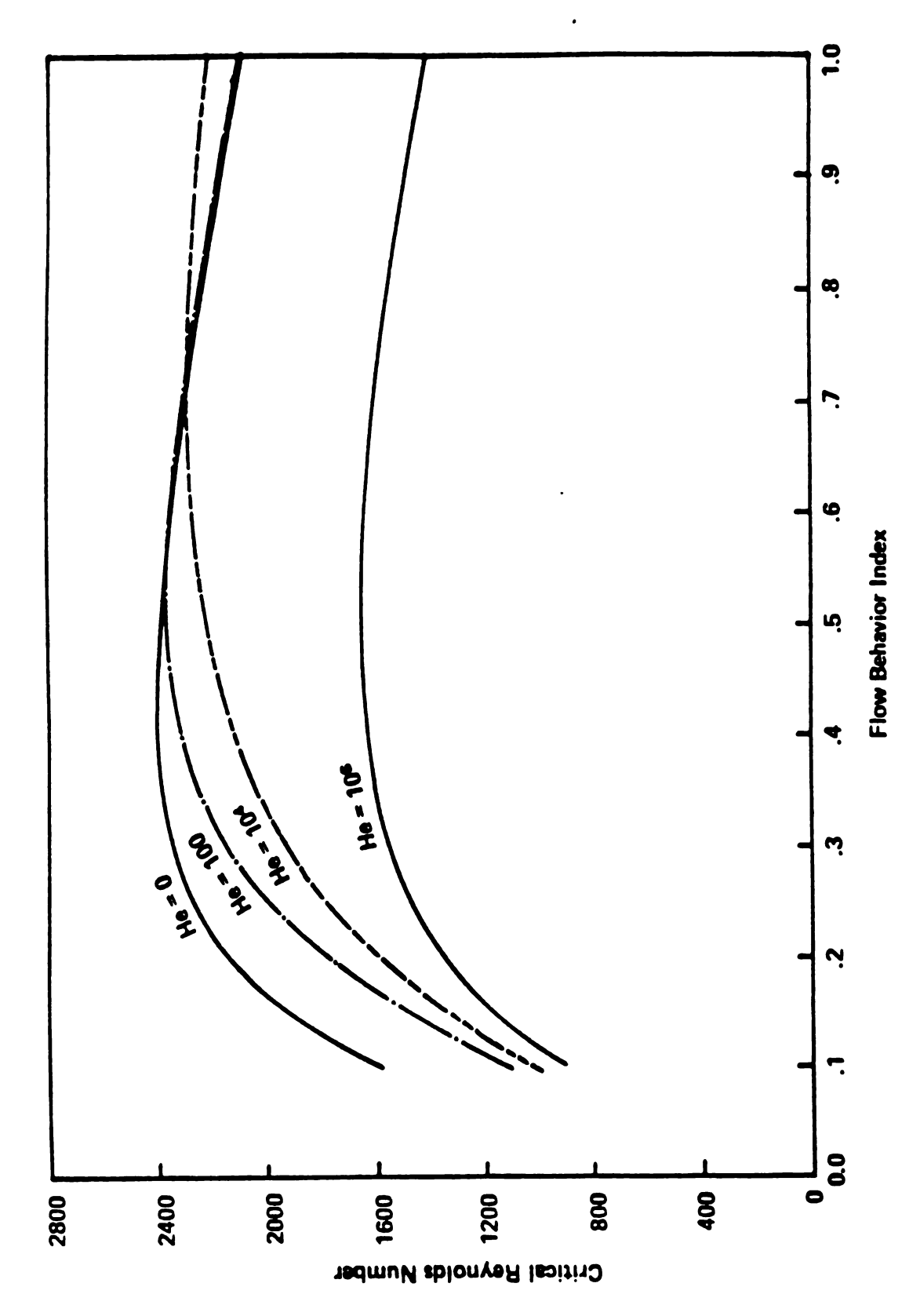


Figure 6. Flow chart showing the calculation scheme to evaluate the critical Reynolds number.



Critical Reynolds number as a function of the Hedstrom number and the flow behavior index. Figure 7.

5. RESULTS AND DISCUSSION

The intent in this study is to show the influence of the precision and magnitude of the rheological parameters on the flow rate calculations. The effect of the magnitude of the parameters will also be discussed. This goal was achieved by assuming hypothetical values for precision and magnitude, then calculating the resulting errors in flow rate. The influence of the pressure drop tube length and diameter were also investigated.

5.1 Pressure Drop and Tube Geometry

To investigate the effect of pressure drop, tube length and tube diameter, all the variables were kept constant while the parameter under consideration was varied. From the computer output, the error of flow rate versus the rheological parameter was obtained. Figure (8) shows contour plot for an error level of 4.1% in flow rate for three values of pressure drop. This plot was selected from other plots for comparison purposes. For pressure drop of 8.0 kPa the error in flow rate is very dependent on the magnitude of the yield stress. As the magnitude of the pressure drop increased, the error tends to be less dependent on the magnitude of the yield stress. This trend occurs because of the direct relationship betwen the shear stress at the wall and the pressure drop. As the shear stress at the wall increases, relative to the yield stress, the contribution to total flow from the unsheared plug flow (which is a function of the yield stress) tends to decrease.

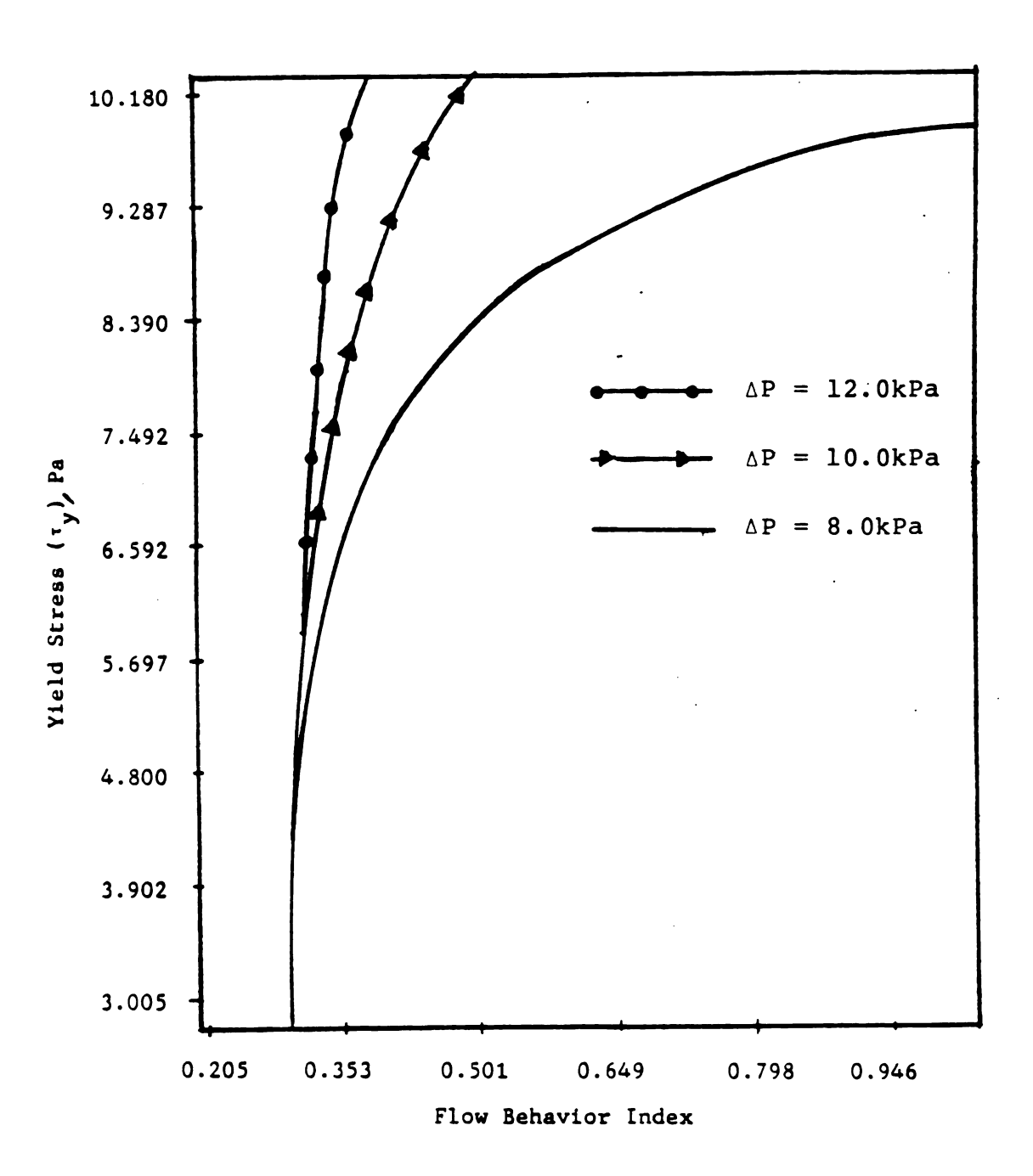


Figure 8. Contour plot of an error of \pm 4.1% in flow rate which results from different values of pressure drop for K = 5.3 Pa·sⁿ, Δ n = \pm 0.0001, Δ K = \pm 1% and Δ τ _y = \pm 0.5%.

Under this condition, the flow rate will be less dependent on the magnitude of the yield stress.

In considering the tube diameter, which is directly related to the shear stress at the wall, similar results are observed (Figure 9). When investigating tube length, which is inversely proportional to the shear stress, the error in flow rate is more dependent on the magnitude of the yield stress as the tube length increases (Figure (10)). The effect of the magnitude of the yield stress and the flow behavior index in generating error in the flow rate calculation may be examined with reference to Figures (9) and (10). Additional discussion will following in the next section.

5.2 Effect of the Yield Stress

The influence of the different precision levels in the yield stress was investigated by varying these levels while all other variables were kept constant. Figures (11) (12) and (13) show the results obtained from the computer output. Results show the dependence of the error on the magnitude of the yield stress. Specially, as the yield stress approaches the shear stress at the wall, the error in flow rate increases because the contribution to the total flow from the plug flow region increases with an increase in the magnitude of the yield stress. Increasing the error in the yield stress from \pm 0.5% to \pm 3.0%, increases the error in flow rate from \pm 9.2% (for τ_y = 9.2 Pa, K = 5.3 Pa s and n = .25) to \pm 50% (for τ_y , K and n equal to the same values) as

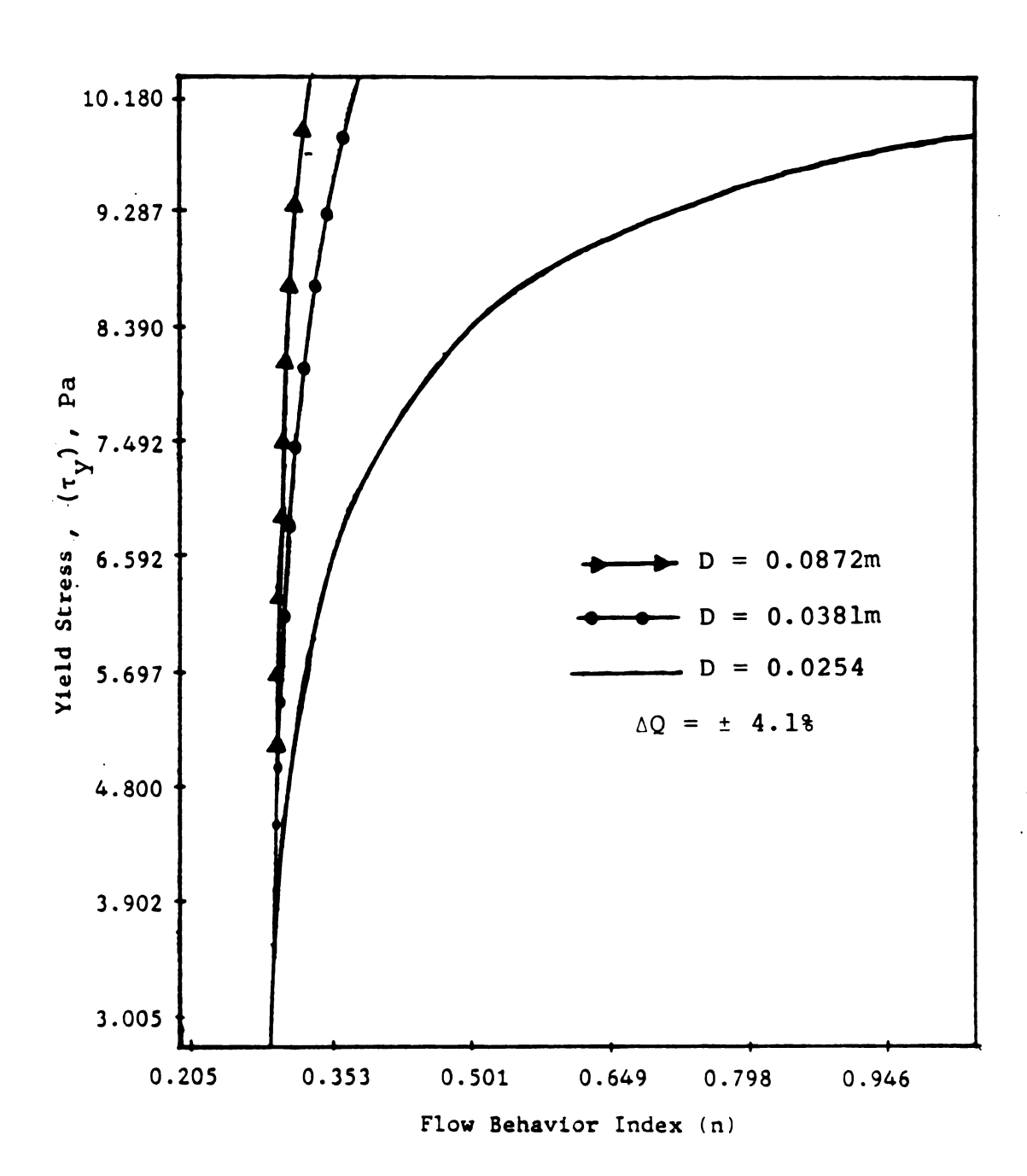


Figure 9. Contour plot of an error of \pm 4.1% in flow rate which results from different values of pipe diameter for K = 5.3 Pa·sⁿ, $\Delta n = \pm$ 0.0001, $\Delta K = \pm$ 1.0% and $\Delta \tau_y = 0.5$ %.

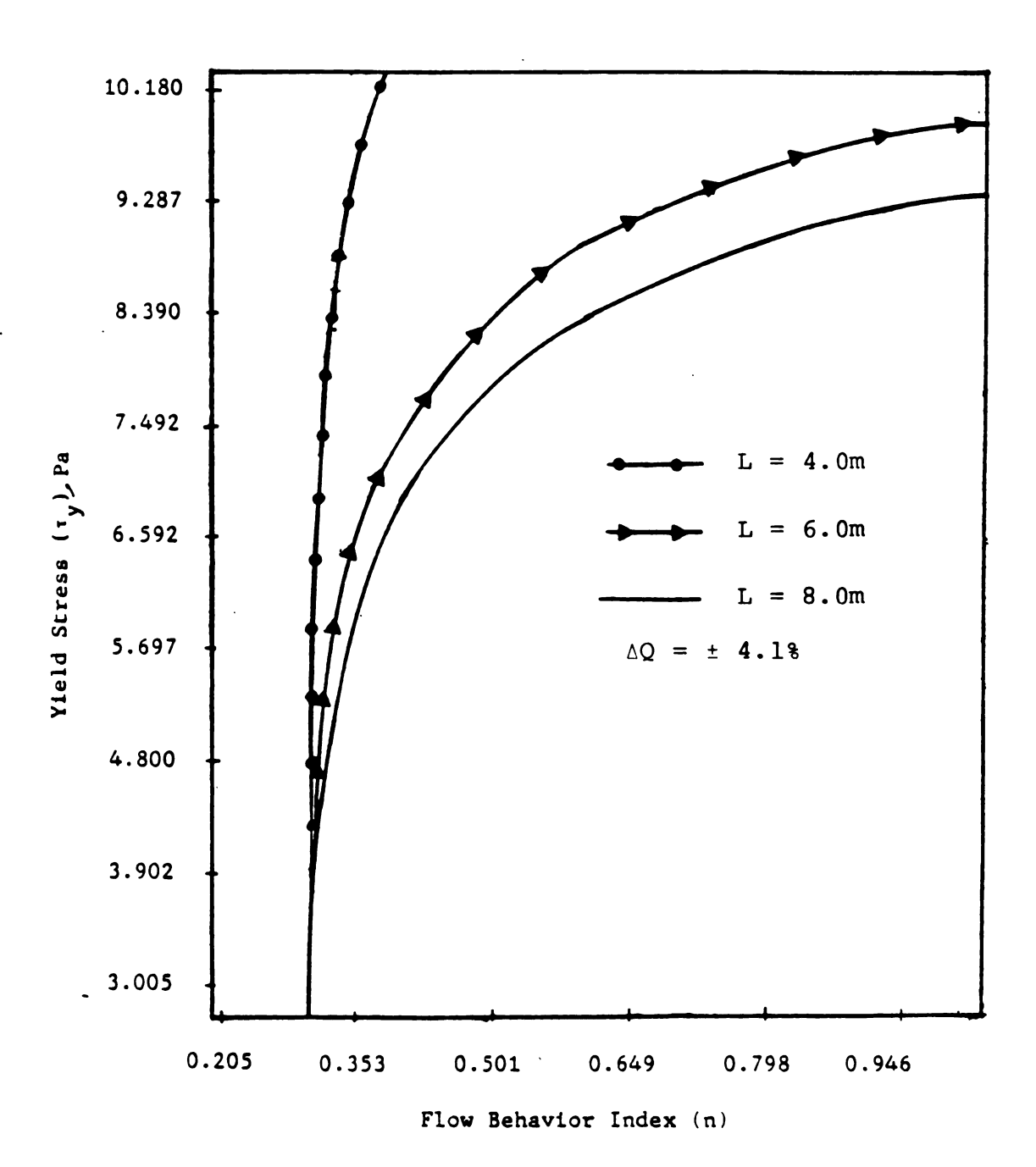


Figure 10. Contour plot of an error of \pm 4.1% in flow rate which results from different values of pipe length for K = 5.3 Pa·sⁿ, $\Delta n \pm 0.0001$, $\Delta K = \pm 1.0$ % and $\Delta \tau_{y} = \pm 0.5$ %.

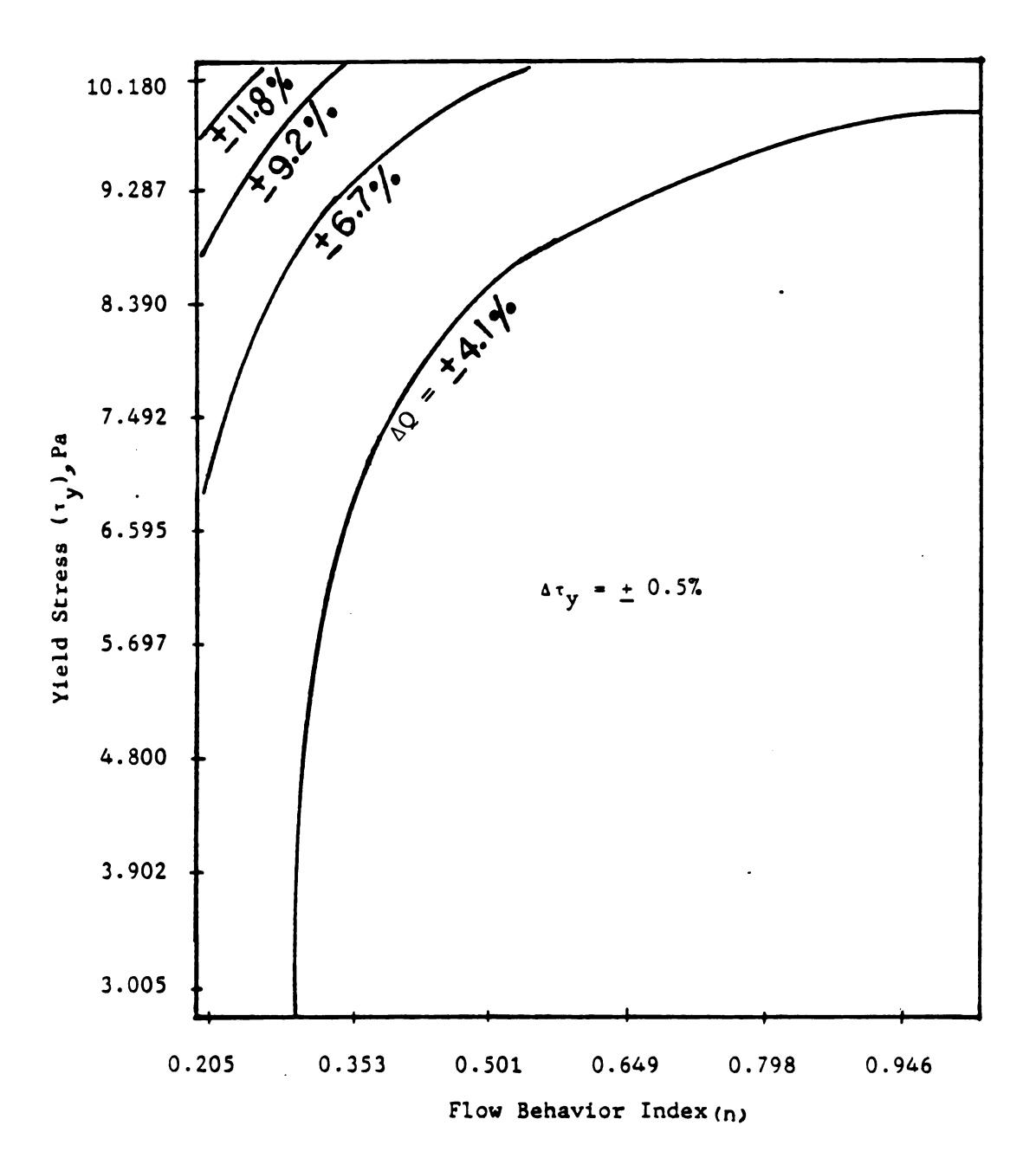


Figure 11. Percentage error in flow rate as a function of the yield stress, and flow behavior index for K = 5.3 Pa·sⁿ, Δn = \pm 0.0001, ΔK = \pm 1.0% and $\Delta \tau_{y}$ = \pm 0.5%.

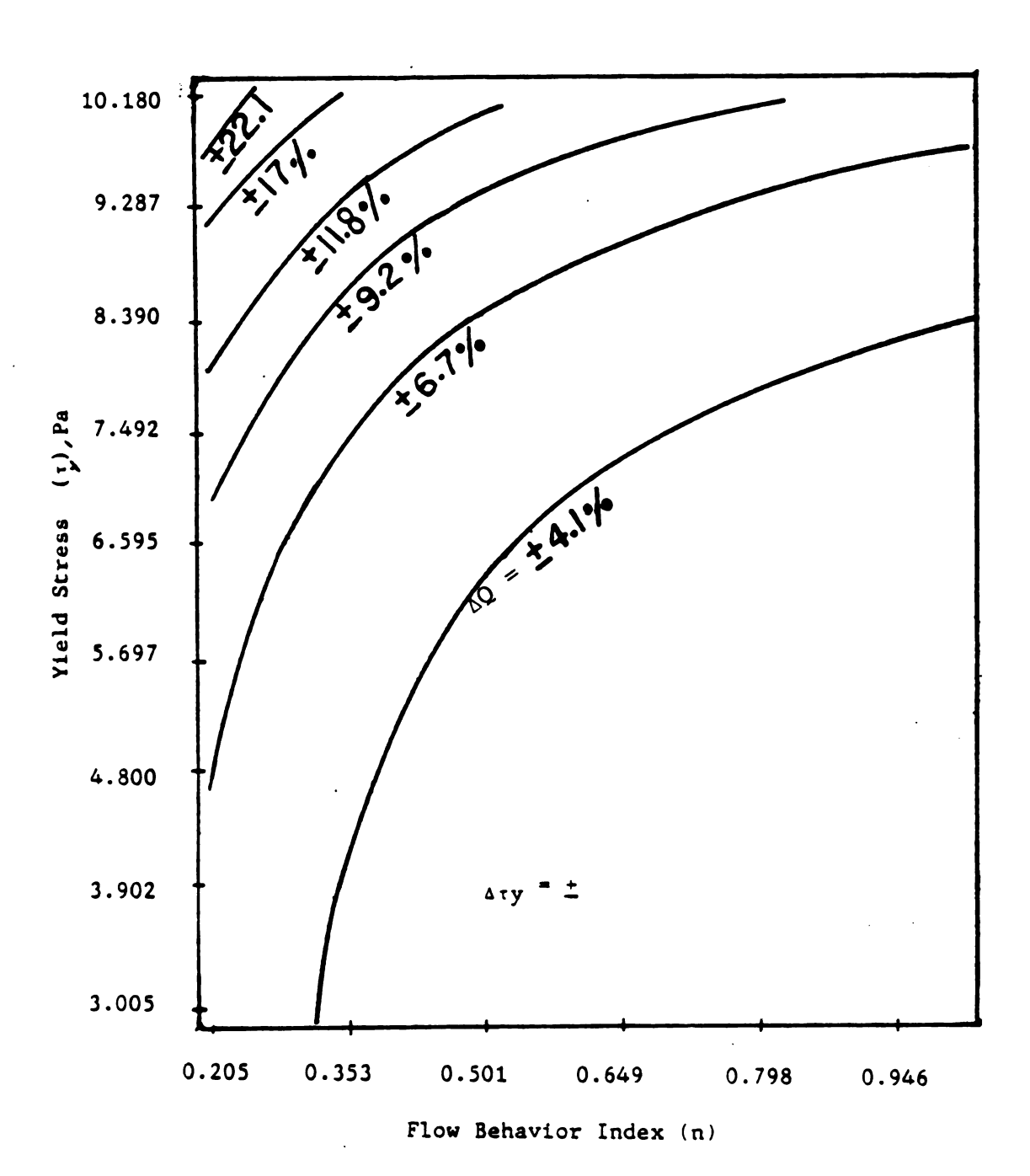


Figure 12. Percentage error in flow rate as a function of the yield stress and flow behavior index for K = 5.3 Pa·sⁿ, $\Delta n = \pm 0.0001$, $\Delta K = \pm 1.0$ % and $\Delta \tau_y = \pm 1.0$ %.

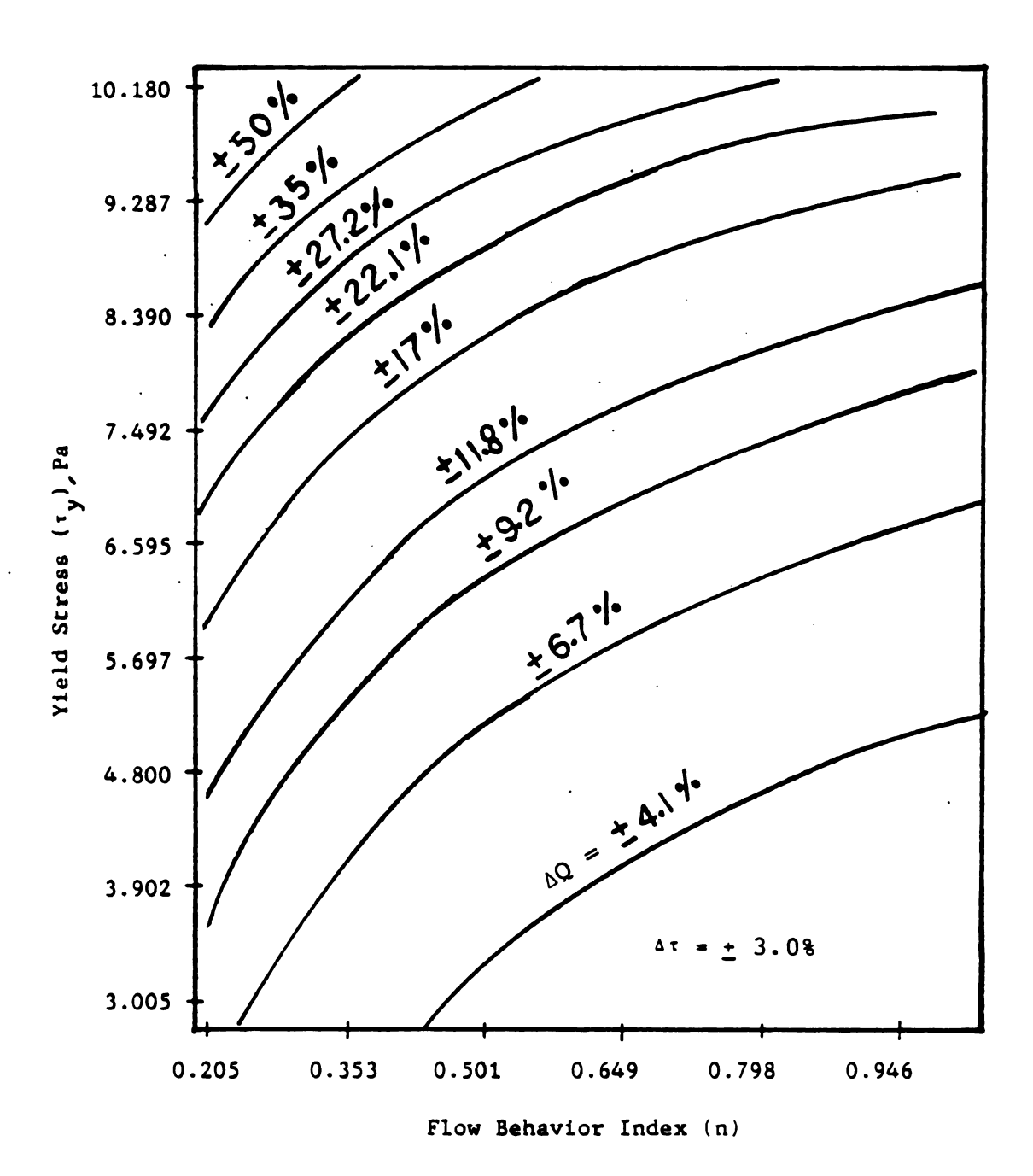


Figure 13. Percentage error in flow rate as a function of the yield stress and flow behavior index for K = 5.3 Pa·sⁿ, Δn = ± 0.0001, ΔK = ± 1.0% and $\Delta \tau_y$ = ± 3.0%.

illustrated in (Figures (11) and (13).

5.3 Effect of the Consistency Coefficient

The influence of the magnitude of the consistency coefficient is illustrated by considering plots of the error in the flow rate viewed against the consistency coefficient and the flow behavior index. The effect of precision level is shown in Figures (14), (15) and (16). The error in flow rate does not change significantly with the magnitude of the consistency coefficient; however, an increase of the levels of the error in consistency coefficient produces some changes in flow rate error.

To compare the error from the consistency coefficient to that from the yield stress, consider Figures (13) and (16) which have errors of \pm 3% in yield stress and consistency coefficient respectively. If the value of the yield stress is 7.67 Pa and the value of n is 0.32, then from Figure (13) the error in flow rate would be \pm 20% (for $\Delta \tau_{y} = \pm$ 3%) compared to \pm 11.8% (for $\Delta K = \pm$ 3%) from Figure (16). Hence, the flow rate is more sensitive to the error in the yield stress, than error in the consistency coefficient.

5.4 Effect of the Flow Behavior Index

The error in flow rate was presented as a function of the flow behavior index and the yield stress or the consistency coefficient for all the Figures (8) through (18). The error in flow rate always increases with decreases in the flow behavior index. For considering the

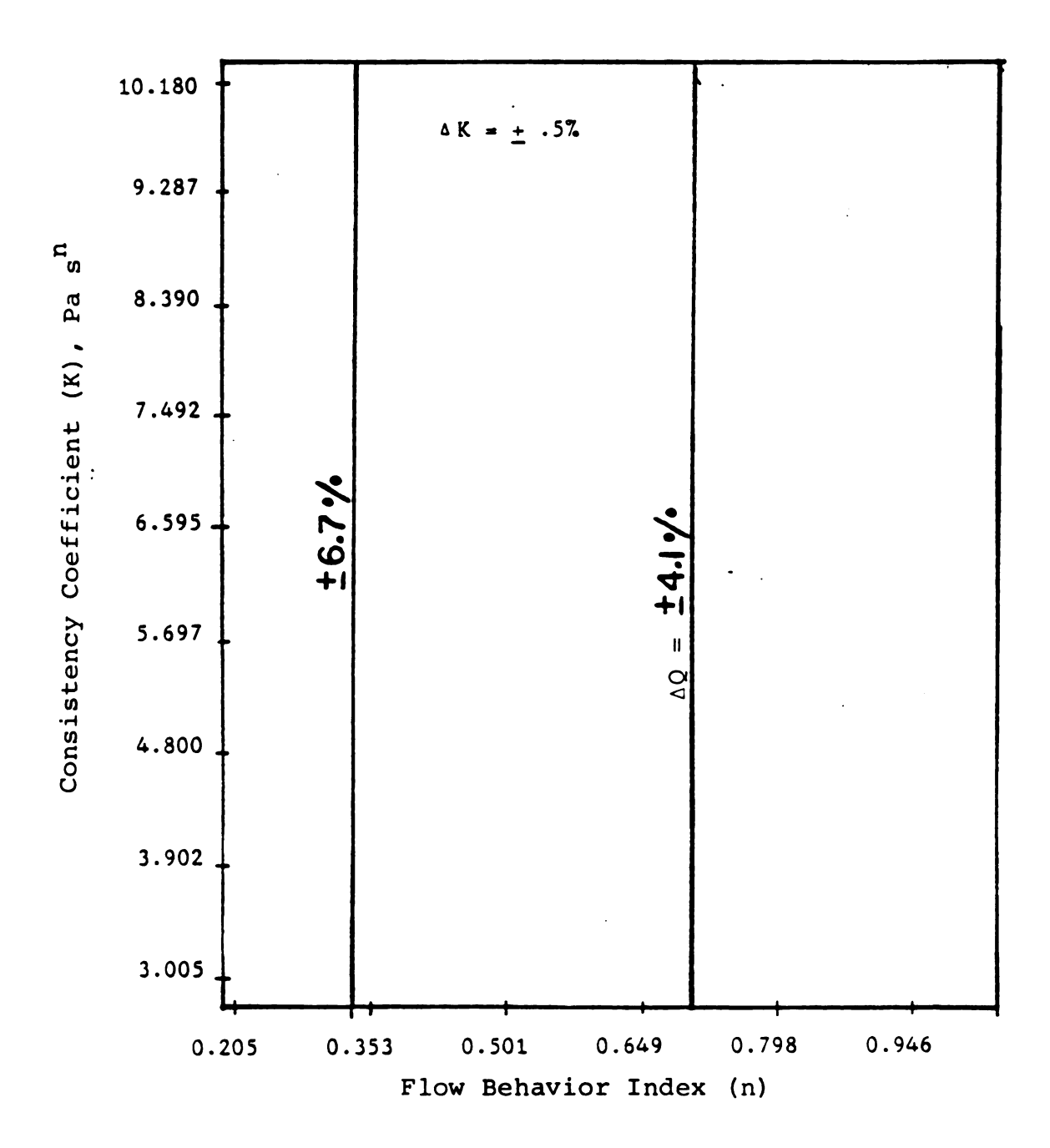


Figure 14. Percentage error in flow rate as a function of the consistency coefficient and flow behavior index for τ_y = 7.67 Pa, Δn = \pm 0.0001, ΔK = \pm 0.5% and $\Delta \tau_y$ = \pm 1.0%.

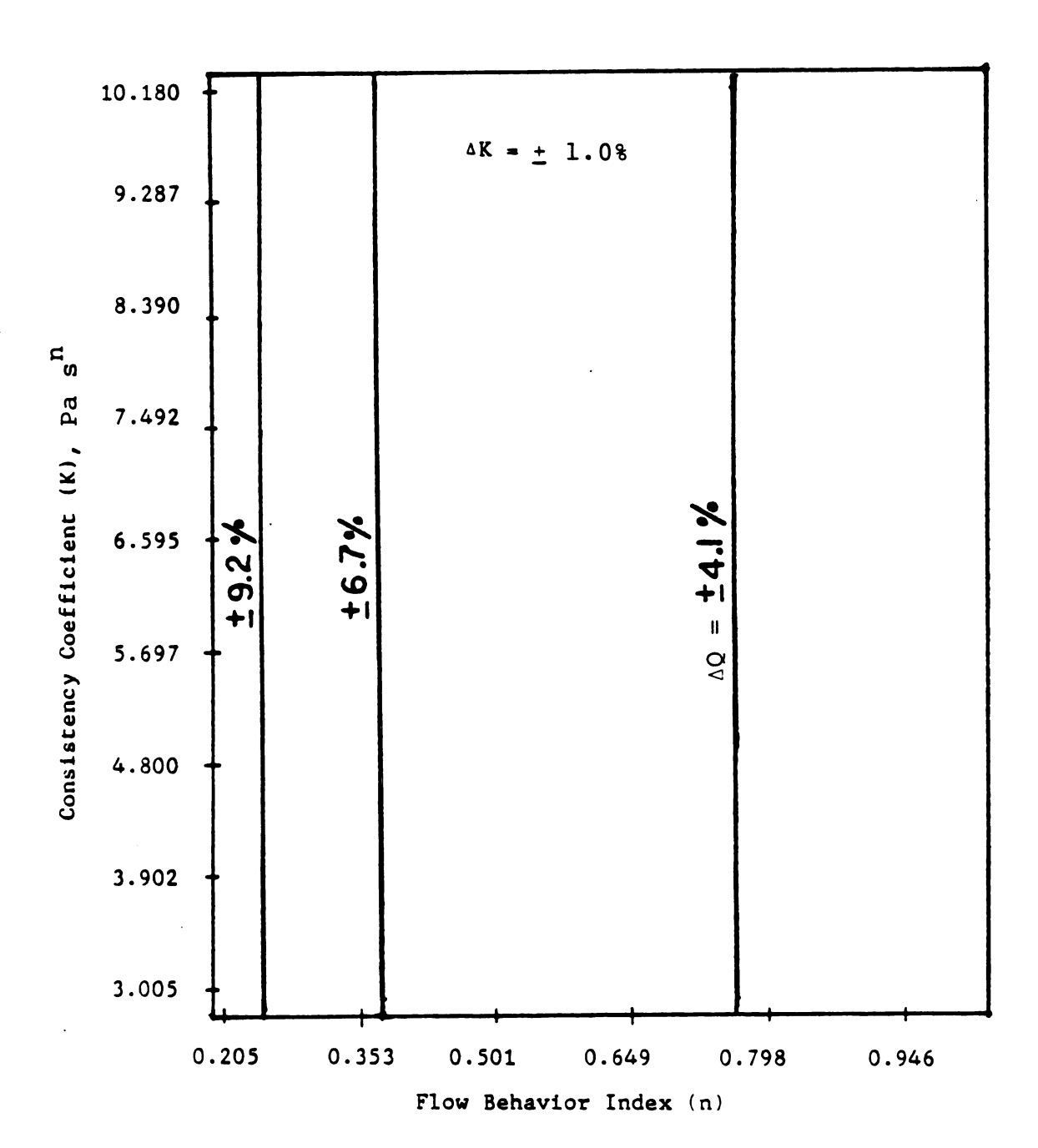


Figure 15. Percentage error in flow rate as a function of the consistency coefficient and flow behavior index for τ_{y} = 7.67 Pa, Δn = ± 0.0001, ΔK = ± 1.0% and $\Delta \tau_{y}$ = 1.0%.

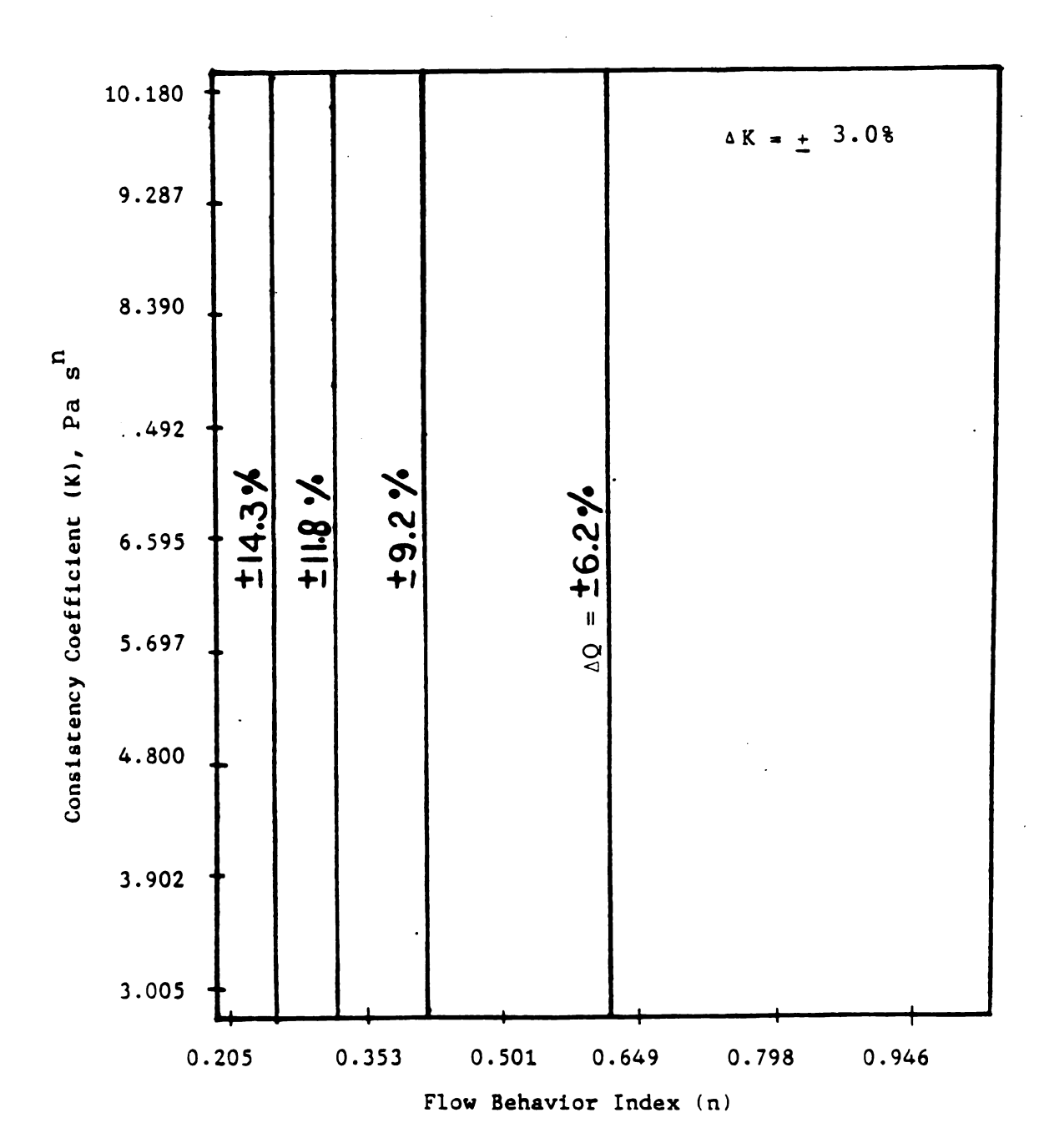


Figure 16. Percentage error in flow rate as a function of the consistency coefficient and flow behavior index for τ_y = 7.67 Pa, Δn = ± 0.0001, ΔK = ± 3.0% and $\Delta \tau_y$ = ± 1.0%.

effect of different precision levels, results are presented in Figures (13), (17) and (18). The results show no significant influence on flow rate over the precision levels investigated. This may be due to the fact that small changes in the n value will not affect the velocity profile in the area where the yield stress has not been exceeded. A similar conclusion was reached by Dodge and Metzner (1959) for the turbulent flow of pseudoplastic fluids for which the velocity profile is quite flat near the center of the tube. They stated that "for pseudoplastic fluids the mean velocity is relatively insensitive to any variation in the n value in the low shear stress region near the center of the tube."

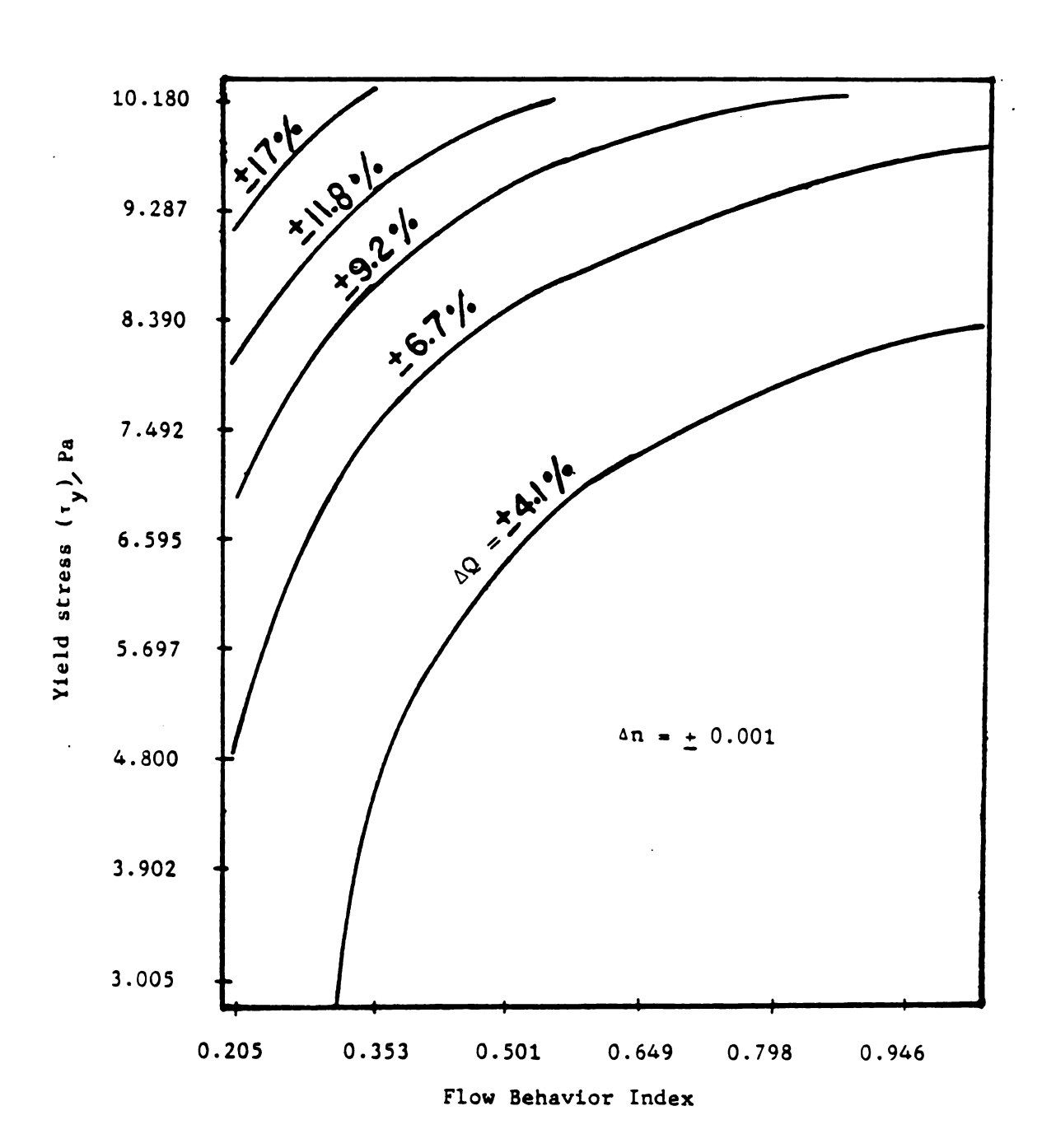


Figure 17. Percentage error in flow rate as a function of the yield stress and flow behavior index for K = 5.3 Pa·sⁿ, $\Delta n = \pm 0.01$, $\Delta K = \pm 1.0\%$ and $\Delta \tau_y = \pm 1.0\%$.

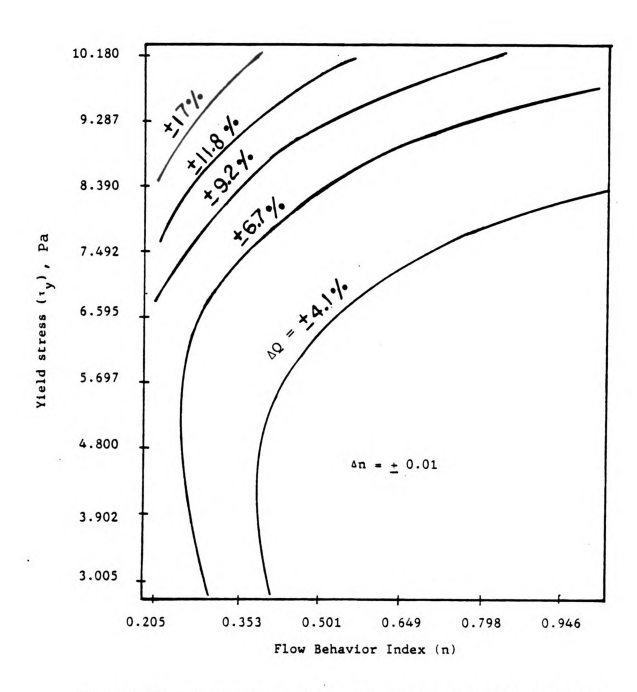


Figure 18. Percentage error in flow rate as a function of the yield stress and flow behavior index for K = 5·3 Pa·s $^{\Pi}$, Δn = \pm 0.01, ΔK = \pm 1.0% and $\Delta \tau_{Y}$ = \pm 1.0%.

6. CONCLUSIONS

This analysis is intended to demonstrate some of the problems that might be encountered when unreliable rheological data are used to predict flow rate. Published data may be inaccurate due to various factors such as the type of viscometer used, violations of stated or implied assumptions or limitations in the analytical techniques employed. The Herschel-Bulkley fluid model and the root sum square error formula was used in this study to investigate the effect of error in the rheological parameters on flow rate calculations. Based on the results obtained from the analysis, the following specific conclusions may be stated:

- 1. The Hanks and Ricks (1974) model describing the laminartransition and flow provides the best criterion available in published literature for determining a critical Reynolds number for non-Newtonian fluids.
- 2. When the shear stress at the wall is much greater than the yield stress, the error in flow rate is not strongly dependent on the yield stress; however, as the shear stress approaches the yield stress, the error tends to be strongly dependent on the magnitude of the yield stress.
- 3. The error in flow rate increases with increasing measurement error (decreasing precision) in yield stress.
- 4. The error in flow rate is not affected by the magnitude of the consistency coefficient but increased error in

the level of the consistency coefficient (precision error) produced increased error in the calculated flow rate.

5. The error in flow rate tends to increase for all cases investigated with a decrease in the magnitude of the flow behavior index; however, increasing the error level of the flow behavior index did not produce any significant change in flow rate error.

7. REFERENCES

- Benson, S.W. 1960. The Fundamentals of Chemical Kinetics. Ch. 4 in "Phenomenological Description of Rates," P. 86. McGraw-Hill, New York.
- Boger, D.C., Tiu, C. 1974. Rheological Properties of Food Products and Their Use in the Design of Flow System. Food Technol. in Australia. 26:325.
- Bongenaar, J.J.T.M., Kossen, N.W., Metz, B., and Meijboom, F.W. 1973. A method for characterizing the rheological properties of viscous fermination broth. Biotech. Bioeng. XV:201.
- Charm, S.E. 1963. The direct determination of shear stress, shear rate behavior of food in the presence of yield stress. J. Food Sci. 28:107.
- Charm, S.E. 1963. Effect of the yield stress on the power law constant of fluid food material determined in law shear rate viscometer. I and EC Process Design and Development. 2:62.
- Cheng, D.C.H. 1970. A design procedure for pipe line flow of non-Newtonian dispersed systems. In "Proceedings of the First International Conference on the Hydraulic Transport of Solids in Pipes (Hydrotransport 1)," Sept. 1-4. British Hydromechanics Research Association, Cranfield, Bedford, England.
- Dickie, A.M. and Kokini, J.L. 1983. An improved model for food thickness from non-Newtonian fluid mechanics in the mouth. J. Food Sci. 48(1):57.
- Dodge, D.W. and Metzner, A.B. 1959. Turbulent flow of non-Newtonian system. A.I.Ch.E. Journal 5(2):189.
- Hanks, R.W. and Christiansen, E.B. 1962. The laminarturbulent transition in non-isothermal flow of pseudoplastic fluid in tubes. A.I.Ch.E. Journal 8:467.
- Hanks, R.W. 1969. A theory of laminar flow stability. A.I.Ch.E. Journal 15(1):25.
- Hanks, R.W. and Ricks, B.L. 1974. Laminar-turbulent transition in flow of pseudoplastic fluid with yield stress. J. Hydronautic. 8:193.
- Harper, J.C. 1960. Viscometric behavior in relation to evaporation of fruit puree. Food Tech. 14:557.
- Herschel, W.H. and Bulkley, R. 1926. Konsistenzmessungen von gummi-benzollosunge. Kolloid-z. 39:291-300.

- Green, H. 1949. "Industrial Rheology and Rheological Structures." John Wiley, New York.
- Metzner, A.B. and Reed, J.C. 1955. Flow of non-Newtonian fluids correlation of the laminar, transition, and turbulent-flow regions. A.I.Ch.E. Journal 1(4):434.
- Metzner, A.B. and Otto, R.E. 1957. Agitation of non-Newtonian fluids. A.I.Ch.E. Journal. 3:3.
- Mizrahi, S. and Berk, Z. 1972. Flow behavior of concentrated orange juice mathmatical treatment. J. of Texture Studies. 3:69.
- Mooney, M. 1931. Explicit formulas for slip and fluidity. J. Rheol. 2:210.
- Nakayama, T., Niwa, E. and Hamada, I. 1980. Pipe transportation of minced fish paste. J. Food Sci. 45:844.
- Odigboh, E.U. and Mohsenin, N.N. 1974. Effect of concentration of the viscosity profile of cassava starch paste during cooking-cooling process. J. of Texture Studies. 5:441.
- Rabinowitsch, B. 1929. Uber die viskosital und elastizitat von salen. Z. Physik. Chem. 145A,1.
- Rao, M.A. 1975. Measurement of flow properties of food suspension with a mixer. J. of Texture STudies, 6:533.
- Rao, M.A. 1977. Rheology of liquid foods a review." J. of Texture Studies 8:135.
- Rao, M.A., Bourne, M.C. and Cooley, H.J. 1981. Flow properties of tomato concentrate. J. of Texture Studies, 12:521.
- Rao, V.N.M., Hamann, D.D. and Humphries, E.G. 1975. Flow behavior of sweet potato puree and its relation to mouth feel quality. J. of Texture Studies, 6:197.
- Ryan, N.W. and Johnson, M.M. 1959. Transition for laminar to turbulent flow in pipes. A.I.Ch.E. Journal 5(4):433.
- Saravacos, G.D. and Moyer, J.C. 1967. Heating rates of fruit products in agitated kettle. Food Tech., 21:372.
- Scarbrough, J.B. 1966. "Numerical Mathematical Analysis." 6th Ed. The Johns Hopkins Press, Baltimore.

- Skelland, A.H.P. 1967. "Non-Newtonian Flow and Heat Transfer." John Wiley and Sons, Inc., New York.
- Steffe, J.F., Mohamed, I.O. and Ford, E.W. 1983.
 Rheological properties of fluid food. Paper No. 83-6512. American Society of Agricultural Engineers, St. Joseph, Michigan.
- Van Wazer, J.R., Lyons, J.W., Kim, K.Y. and Calwell, R.E. 1963. "Viscosity and Flow Measurement." Interscience Publisher, New York.

:	•			
1				
			÷	
1				

